

## Meccano on the Nanoscale—A Blueprint for Making Some of the World's Tiniest Machines

Amar H. Flood,<sup>A</sup> Robert J. A. Ramirez,<sup>A</sup> Wei-Qiao Deng,<sup>B</sup> Richard P. Muller,<sup>B</sup> William A. Goddard III,<sup>B</sup> and J. Fraser Stoddart<sup>A,C</sup>

<sup>A</sup> California NanoSystems Institute, Department of Chemistry and Biochemistry, University of California, Los Angeles, CA 90095-1569, USA.

<sup>B</sup> Materials and Process Simulation Centre, Division of Chemistry and Chemical Engineering, California Institute of Technology, Pasadena, CA 91125, USA.

<sup>C</sup> Author to whom correspondence should be addressed (e-mail: stoddart@chem.ucla.edu).

Molecular compounds—comprised of mechanically interlocked components—such as rotaxanes and catenanes can be designed to display readily controllable internal movements of one component with respect to the other. Since the weak noncovalent bonding interactions that contribute to the template-directed synthesis of such compounds live on between the components thereafter, they can be activated such that the components move in either a linear fashion (rotaxanes) or a rotary manner (catenanes). These molecules can be activated by switching the recognition elements off and on between components chemically, electrically, or optically, such that they perform motions reminiscent of the moving parts in macroscopic machines. This review will highlight how the emergence of the mechanical bond in chemistry during the last two decades has brought with it a real prospect of integrating a bottom-up approach, based on molecular design and micro- and nanofabrication, to construct molecular electronic devices that store information at very high densities using minimal power. Although most of the research reported in this review on switchable catenanes and rotaxanes has been carried out in the context of solution-phase mechanical processes, recent results demonstrate that relative mechanical movements between the components in interlocked molecules can be stimulated (a) chemically in Langmuir and Langmuir–Blodgett films, (b) electrochemically as self-assembled monolayers on gold, and (c) electronically within the settings of solid-state devices. Not only has reversible, electronically driven switching been observed in devices incorporating a bistable [2]catenane, but a crosspoint random access memory circuit has been fabricated using an amphiphilic, bistable [2]rotaxane. The experiments provide strong evidence that switchable catenanes and rotaxanes operate mechanically in a soft-matter environment and can withstand simple device-processing steps. Studies on single-walled carbon nanotubes used as one of the electrodes in molecular switch tunnel junctions have revealed that interfacial chemical interactions involving electrodes containing carbon, silicon, and oxygen are good choices when carrying out molecular electronics on the class of rotaxane- and catenane-based molecules reported in this review. This conclusion is supported by differential conductance measurements (at 4 K) made with single-molecule transistors using the break-junction method. It transpires that the electronic transport properties in such devices are more sensitive to the chemical nature of the molecule–electrode contacts than the details of the molecules' electronic structure away from the contacts. This result has profound implications for molecular electronics and highlights the importance of also considering the molecules and the electrodes as an integrated system. It all adds up to an integrated systems-oriented approach to nanotechnology that finds its inspiration in the transfer of concepts like molecular recognition from the life sciences into materials science and provides a model for how, in principle, to transfer elements of traditional chemistry to technology platforms that are being developed on the nanoscale. Before there can be any serious prospect of a technology, there has to be some good, sound science in the making. Molecular electronics is very much in its infancy and, as such, it can be expected to give rise to a great deal of intellectually stimulating science before it stands half a chance of becoming a viable companion to silicon-based technology.

Manuscript received: 8 December 2003.

Final version: 1 March 2004.

### Introduction

#### *The Future of Technology—Molecular Machinery*

When considering the world's machines, a wide variety of examples, both artificial and natural, can be identified that

span a range of length scales. For example, we think of trains on the order of a kilometer, aircraft carriers down to hundreds of meters, microelectromechanical systems (MEMS) based cogs and gears, reaching down to millimeters, and motor proteins, such as kinesin and ATP-synthase, operating in the

micrometer to sub-micrometer ranges. Artificial machines have been developed by top-down miniaturization, leading ultimately to the nanometer and the domain of single, or ensembles, of molecules. It is from this position that the modern machinist<sup>[1,2]</sup> of ultra-small devices may begin with molecular machinery. Recent demonstrations of wholly synthetic molecular machines include rotary motors,<sup>[3,4]</sup> a rotary motor displaying net unidirectional motion,<sup>[5]</sup> and linear motors.<sup>[4]</sup>

A machine on any length scale should be capable of performing an action (leading to a desired function) by consuming energy, following the input of a signal.<sup>[6]</sup> In the context of a molecule, these machines cannot be held in our hands or seen by our eyes. It is as though humanity, in the guise of Gulliver, enlists the help of the Lilliputians and

asks of them to meld the world 'from invisible thread with invisible needles'. Fortunately, since the time of Jonathan Swift's fiction in 1726, the field of chemistry has marched steadily onwards, such that it has now reached a time where all of its traditional elements can be brought to bear on the construction, manipulation, and visualization of molecular machinery.

As a caveat to the analytical acuity that characterizes modern chemical research, forays into new fields, such as in molecular electronics, require an approach that acknowledges the fact that the structures and dynamics of molecules veiled behind electrodes are far from easy to characterize in electronic devices. Consequently, the appropriate control studies need to be performed. In particular, the influence of *switchable* and *nonswitchable* compounds on the observable



*Amar H. Flood was born in Napier, New Zealand, in 1974. He received his B.Sc.(Hons) in 1997 from the University of Otago, Dunedin. There, he continued his studies focussing on the chemistry of metal polypyridyl complexes under the supervision of Keith Gordon, graduating with his Ph.D. in 2001. During 1998, he spent a summer as a Claude McCarthy Fellow at the University of York in the UK with Ron Hester and John Moore. In 2001, he joined Fraser Stoddart's group at the University of California, Los Angeles, where he is presently involved, as a research associate, in the development of nanoelectronics and nanoelectromechanical systems.*



*Robert J. A. Ramirez was born in Manila, Philippines, in 1972. He obtained his B.S. and M.S. from California State University, Los Angeles, where he studied under Carlos Gutierrez on the synthesis and NMR spectroscopic behavior of the high-affinity iron chelator, enterobactin. He is currently working towards his Ph.D. with Fraser Stoddart at the University of California, Los Angeles, on the noncovalent functionalization of single-walled carbon nanotubes with pyridyl-containing, transition-metal based cyclophanes.*



*Wei-Qiao Deng was born in Hubei, China, in 1973. He obtained his B.S. from Lanzhou University and M.S. from Dalian Institute of Chemical Physics, where he worked on the state-state reactions by using molecular beams. He is currently carrying out research as a graduate student with William A. Goddard III at the California Institute of Technology on the computation-aided design of molecular nanotechnologies.*



*Richard P. Muller was born in Chicago, USA, in 1966. He received his B.A. (1988) from Rice University, and his Ph.D. (1994) from the California Institute of Technology under the guidance of William Goddard III. After a postdoctoral position at the University of Southern California studying enzyme catalysis with Ariele Warshel, he returned to Caltech where he was a senior scientist in Goddard's research centre, directing the centre's interests in quantum chemistry and catalysis. In 2003, he moved to Sandia National Laboratories in Albuquerque, New Mexico, where he is a senior member of the technical staff in the Computational Materials and Molecular Biology Department. His interests range from software engineering, to quantum chemistry methodology, to photo- and electro-catalysis.*



*William A. Goddard III was born in Imperial Valley, USA, in 1937. He received his B.S. (1960) from the University of California at Los Angeles, and his Ph.D. (1965) from the California Institute of Technology where he has remained since. He is currently the Charles and Mary Ferkel Professor of Chemistry, Materials Science, and Applied Physics and Director of the Materials and Process Simulation Center at the California Institute of Technology. The long-term objective of Professor Goddard's research has been to describe the properties of chemical, biological, and materials systems directly from first principles. He has been named as one of the 99 most Highly Cited Chemists for 1981–1999. He has received many prizes, including the 2002 IMM Prize in Computational Nanotechnology Design from the Institute for Molecular Manufacturing and has been awarded an Honoris Causa Philosophia Doctorem from Uppsala University, Sweden, in January 2004.*



*J. Fraser Stoddart was born in Edinburgh, Scotland, in 1942. He received his B.Sc. (1964), Ph.D. (1966), and D.Sc. (1980) from the University of Edinburgh. A nomadic career, spent briefly in Canada (Queen's University) and then in England (Sheffield University and Birmingham University with a sojourn at the Imperial Chemical Industries Corporate Laboratory in Runcorn), has led him to his present association with the University of California at Los Angeles where he is Director of the California NanoSystems Institute and holds the Fred Kavli Chair in NanoSystems Sciences. He has pioneered the development of molecular recognition-cum-self-assembly processes and template-directed protocols for the syntheses of mechanically interlocked compounds (catenanes and rotaxanes) that have been employed as molecular switches and as motor molecules, respectively, in the fabrication of nanoelectronic and nanoelectromechanical systems. He is the recipient of many including awards most recently, in 2004, the Nagoya Gold Medal in Organic Chemistry.*

phenomena of current flow and voltage thresholds are sometimes the only guiding studies that allow the scientist to understand what is occurring inside a particular molecular electronic device. Although the results obtained and the conclusions drawn may not be as definitive as those that have graced traditional fields of chemistry, where analytical techniques exist already in abundance, the hypothesis testing and the stepwise learning that goes hand-in-hand with this style of investigation is intellectually challenging and no less attractive for its ambiguity. Insight and understanding by exploration comes at the cost of certainty.

According to Moore's Law, by 2012 silicon may not be able to meet the requirements of computer technology in terms of manufacturability and operational performance, not to mention spiralling costs. The anticipation of this limitation has led researchers in academia and industry alike to consider alternatives such as the development of nano-electronic devices, based on molecular scale switches.<sup>[7–17]</sup> Although most of these endeavours utilize molecules, some efforts have also been focussed toward the fabrication of

nanowires with a wide variety of structures in terms of doping levels, lengths, widths, concentric rings, and alternating materials, which, although they carry an elegant array of electronic functions,<sup>[18,19]</sup> lack the grace of the rich mechanical structure inherent in a molecule. The simplest devices that can be conceived consist of a crossbar of two electrodes between which are sandwiched molecular switches.<sup>[20–22]</sup> This conception was fulfilled when an electrically switchable molecule—a bistable [2]catenane—was placed between a Si bottom electrode, replete with its native oxide, and a Ti/Al top electrode.<sup>[7]</sup>

### The Development of Molecular Machinery

The realization of such a switchable molecule in a device setting was, however, the culmination of a long period of fundamental research (Fig. 1). Molecular switches developed along a timeline that began in 1978 with simple molecular recognition systems that directed the self-assembly of guests noncovalently bound inside ring-based hosts.<sup>[23]</sup> On

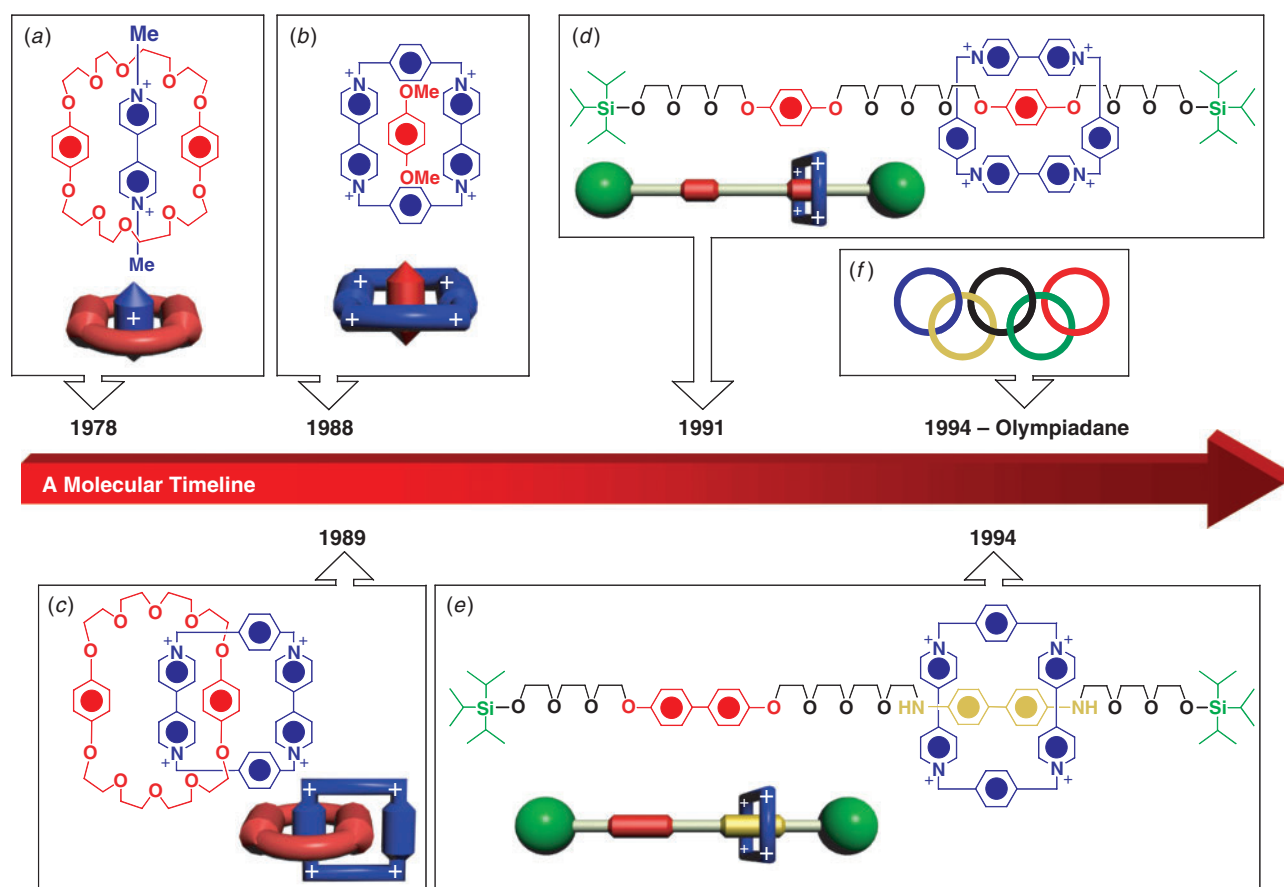


**Fig. 1.** A timeline illustrating the early phase of molecular evolution that led to the design and synthesis of motor molecules, commencing from simple beginnings in host–guest chemistry where (a) the  $\pi$ -acceptor guest is hosted by an electron-rich ring, and (b) the reverse, where the  $\pi$ -acceptor forms the basis for a ring that recognizes aromatic-donor compounds and led to mechanically interlocked molecules. (c) The first catenane to be assembled evolved around the mutual recognition of donor and acceptor aromatic systems, a common motif that was also expressed in rotaxanes. (d) In the first rotaxane, the degeneracy of the two hydroquinone units in the dumbbell component formed a molecular shuttle, and in the situation (e) where one of the two donor units can be readily protonated, a pH or electrochemically driven molecular switch was produced. The mutual recognition motif was taken to a penultimate, yet most culturally appealing expression, in the template-directed synthesis of the [5]catenane, dubbed Olympiadane. By stepping back from this level of topological complexity, the opportunity came to develop the switching character into a series of motor molecules that found their initial calling at the nanoscale level in electronic devices.

the back of the rapidly developing field of supramolecular<sup>[24–26]</sup> and host–guest chemistry<sup>[25,27]</sup> came a mechanically interlocked compound in 1989 called a donor–acceptor catenane.<sup>[28]</sup> This compound was prepared efficiently<sup>[27]</sup> using hydroquinone donor units within a macrocyclic polyether, bisparaphenylene[34]crown-10 (BPP34C10) as the template to direct the synthesis of a tetracationic cyclophane, cyclobis(paraquat-*p*-phenylene) (CBPQT<sup>4+</sup>). In this manner, the two ring-shaped components—BPP34C10 and CBPQT<sup>4+</sup>—become interlocked together. In the solution phase, it was observed, using variable-temperature <sup>1</sup>H NMR spectroscopy, that neither one of the two rings are ever motionless. On the contrary, these two rings are constantly circumrotating through each other's cavities, with pauses, when the paraquat acceptor and the hydroquinone donor units recognize each other's attractive interactions, which also include strong (C–H···O) and weak (C–H···π) interactions. This constant motion can only be quenched as the temperature is lowered, allowing the array of noncovalent bonds to persist between each donor and acceptor pair.

The facility and ease with which a [2]catenane could be made proffered the challenge to template the synthesis of catenanes with a larger number of interlocked rings. Success was found<sup>[29]</sup> reasonably easily by using larger rings composed of multiple donor/acceptor recognition sites to produce ultimately, in a hyperbolic expression of template-directed synthesis, a [7]catenane. However, perhaps even more aesthetically appealing, a [5]catenane was isolated that displays the same interlocking sequence of five rings as evident in the Olympic symbol—hence the name Olympiadane was claimed for the compound.

Notwithstanding the simplicity with which these higher catenanes were prepared—the five interlocked rings of Olympiadane, obtained in an astounding 30% yielding reaction—the corresponding rotaxane-based versions of these systems were designed and synthesized. [2]Rotaxanes bear only one ring-shaped component that is mechanically interlocked around a dumbbell-shaped component.<sup>[30]</sup> To maintain this ring in place around the dumbbell, bulky stoppering groups are attached to the ends of the rod section of the dumbbell. In keeping with the [2]catenanes, hydroquinone donor units, placed along the dumbbell's length, serve as the recognition sites around which to template the formation of the CBPQT<sup>4+</sup> ring, can be templated by the dumbbell component. Faced again with a system<sup>[31]</sup> that is in constant motion—the CBPQT<sup>4+</sup> ring shuttles back and forth between the identical hydroquinone donor units by overcoming a 13 kcal mol<sup>-1</sup> activation barrier—it became pertinent to exercise dominion over these ceaseless motions, enforcing control over the CBPQT<sup>4+</sup> ring's location by employing stronger donors. Moreover, when the two donors are different, it is possible to create a switchable bistable [2]rotaxane—such is the case with the benzidine and biphenol units that define a pH and electrochemically switchable rotaxane.<sup>[32]</sup> Although the starting state in this system suffered the inconvenience of constant shuttling, once protons are added to, or electrons are removed from, the benzidine unit, its recognition properties are instantly nullified and

hence the CBPQT<sup>4+</sup> ring promptly localizes itself around the biphenol unit. The rotaxane can be switched back again to its starting state by adding base or electrons to the system. From this first example, molecular switches developed apace by focussing the emphasis upon their optimization and customization.

Since the early 1990s many other switchable catenanes and rotaxanes have been developed and modified systematically. In our own laboratories, we have developed electrically stimulated bistable switches that afford us a high degree of control over the equilibrium location of the two components—indeed, to such an extent that only one of the two translational isomers is observed. For example,<sup>[33]</sup> a [2]catenane (Fig. 2a), in which a crown ether component bearing tetrathiafulvalene (TTF) and 1,5-dioxynaphthalene (DNP) recognition stations is interlocked within the CBPQT<sup>4+</sup> ring, exists as only one stable translational isomer—namely, the one on which the TTF unit resides inside the CBPQT<sup>4+</sup> ring with the DNP ring system outside. This catenane, first characterized in solution using cyclic voltammetry (CV), shows a departure from standard electrochemical behaviour. In the oxidation region normally associated with the TTF unit, wherein the simple thread-shaped compound (Fig. 2b) shows two fully reversible one-electron oxidation processes, the CV changes its shape in a way that can be explained on the basis of the molecular structure. The position of the first oxidation peak shifts 230 mV to more positive potentials as a consequence of the TTF unit's localization inside the tetracationic cavity of the π-electron poor CBPQT<sup>4+</sup> ring. However, the second oxidation peak occurs at the same potential as that observed for the simple thread. This observation is consistent with the fast circumrotation of the crown ether component as a result of charge–charge repulsion between the CBPQT<sup>4+</sup> ring and the now-charged monocationic TTF<sup>+</sup> unit. Once the neutral form of the TTF unit is re-established at potentials more negative than 360 mV, the crown ether component circumrotates back to its original starting position. In this manner, the catenane can be switched oxidatively between one of its two bistable states, in which either the TTF or the DNP unit is inside the CBPQT<sup>4+</sup> ring's cavity.

Analogous bistable catenates and metallated rotaxanes, which can be electrochemically activated, have been developed that are based on the translocation of transition metal ions. For example, Sauvage<sup>[4]</sup> has made effective use of the differences in coordination requirements between copper(I) and copper(II) redox centres. The former prefers a four-coordinate arrangement, whereas the latter likes a five-coordinate environment. An electrochemically active metallated rotaxane<sup>[34]</sup> was prepared wherein the dumbbell component displays, at different locations along its axis, one bidentate and one tridentate polypyridyl ligand. A ring incorporating a bidentate chelating ligand, which in the presence of copper(I) binds selectively to the bidentate site, is threaded onto the dumbbell. Electrochemical oxidation forms the copper(II) state, which causes the translocation of the ring and the copper(II) metal ion from the bidentate to the tridentate site in order to accommodate the five-coordinate bonding requirement of the copper centre. Although such systems have

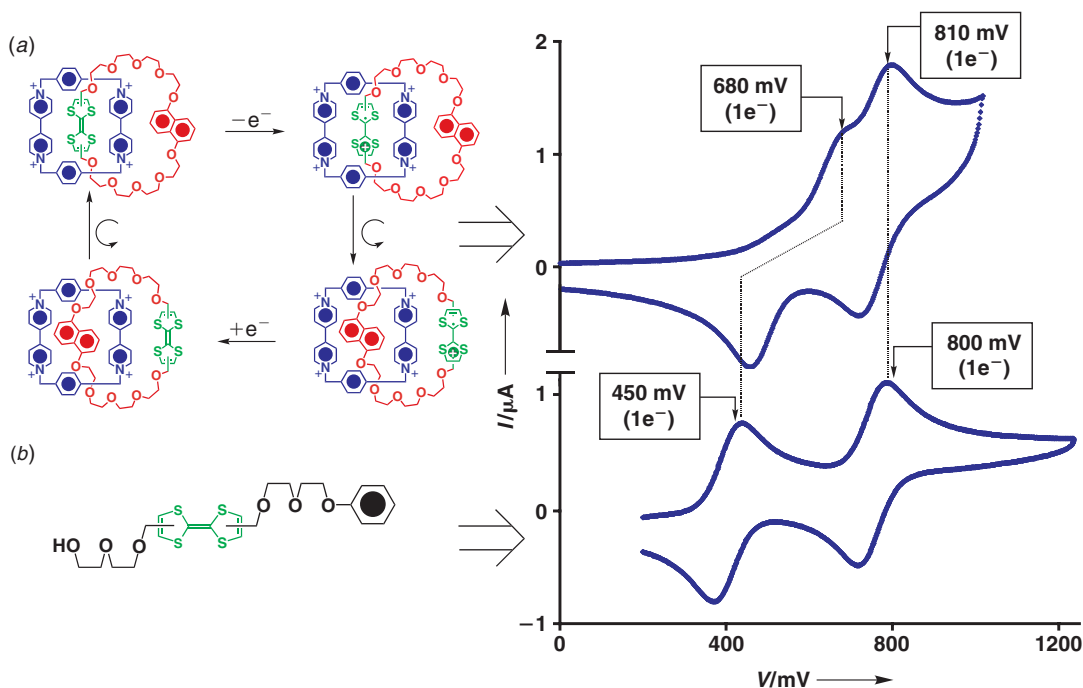


**Fig. 2.** (a) Structural formulas and nanoelectromechanical switching cycle for a bistable [2]catenane beginning in its thermodynamically favoured co-conformer (upper left) with the TTF unit localized inside the cavity of the CBPQT<sup>4+</sup> ring. The corresponding cyclic voltammogram (100 mV s<sup>-1</sup>, 0.1 M TBAPF<sub>6</sub>, MeCN) displays the onset of mono-oxidation of the TTF unit at +680 mV, with a second peak at +810 mV. (b) For comparison, the control compound, a TTF-based thread, displays two well-behaved oxidation processes, with the onset of the first and second oxidation peaks observed at +450 and +800 mV, respectively. The modulation of the TTF unit's first oxidation process to form the cation radical in the CV of the [2]catenane is consistent with the TTF unit's location inside the CBPQT<sup>4+</sup> ring. However, the coincidence of the second peak position between the [2]catenane and the TTF-based thread is indicative of the mono-oxidized TTF<sup>•+</sup> units' circumrotation out of the CBPQT<sup>4+</sup> ring's central cavity on account of charge-charge repulsion before the second oxidation.

been extended to catenanes<sup>[35]</sup> and have also been transferred from the solution phase to self-assembled monolayers on gold surfaces,<sup>[36]</sup> none to date, at least to our knowledge, have been incorporated into full-devices.

The development of the mechanically interlocked class of molecular machines did not proceed in a vacuum. Concept transfer (Fig. 3) from the life sciences into materials science has been used to inspire the use of noncovalent interactions as the main source of molecular recognition to drive self-assembly processes, a combination that finds its ultimate expression in the template-directed synthesis—or supramolecular assistance to covalent-bond formation for the preparation—of mechanically interlocked molecules.<sup>[37]</sup> Another of these natural inspirations derives from the protein-based molecular machines, such as the rotary motor ATP-synthase, and the linear motor activity of actin and myosin found in muscle tissue. Taking heed of these natural paradigms of machinery,<sup>[4]</sup> and indeed of humanity's own artificial creations in the highly technological world of today, is of paramount importance for the development and exploitation of molecular machinery. In essence, can we control and harness the relative molecular motions that occur inside switchable rotaxanes and catenanes? That is, can we shift from solution-state incoherence to coherence and cooperativity in condensed phases to make useful devices? In this way, the objective is not necessarily to search for yet more classical chemical phenomena but, instead, to investigate

and understand at a fundamental level the effects of chemical organization on phenomena that are emergent from the *entire* system, for example the emergence of conduction and switching in electronic devices.

#### Nanoelectronics

In this review we will outline how the traditional elements of chemistry, together with the contemporary ideas of nanoscience and nanotechnology, were brought together in an effort to tunnel under the roadblock at the end of the silicon industry's quest by top-down miniaturization for ever faster computers.

The realization of nanoelectronic devices that are based on molecules delineates one of the many territories where a successful foray into the hybrid top-down/bottom-up frontier might be pursued. With the simple model of the electrode crossbar in mind, the significant developments that have paved the way toward the production of molecular electronic devices based on bistable catenanes and rotaxanes will be outlined from the traditional starting place of the design and synthesis of molecular switches, and their initial characterization in solution, into the interface with solid-state systems. Two approaches will be discussed—one involves forming ordered Langmuir monolayers at the air/water interface and the other the formation of self-assembled monolayers (SAMs) on a gold electrode—from the point of view of both full- and half-device fabrication, respectively. In particular, by using

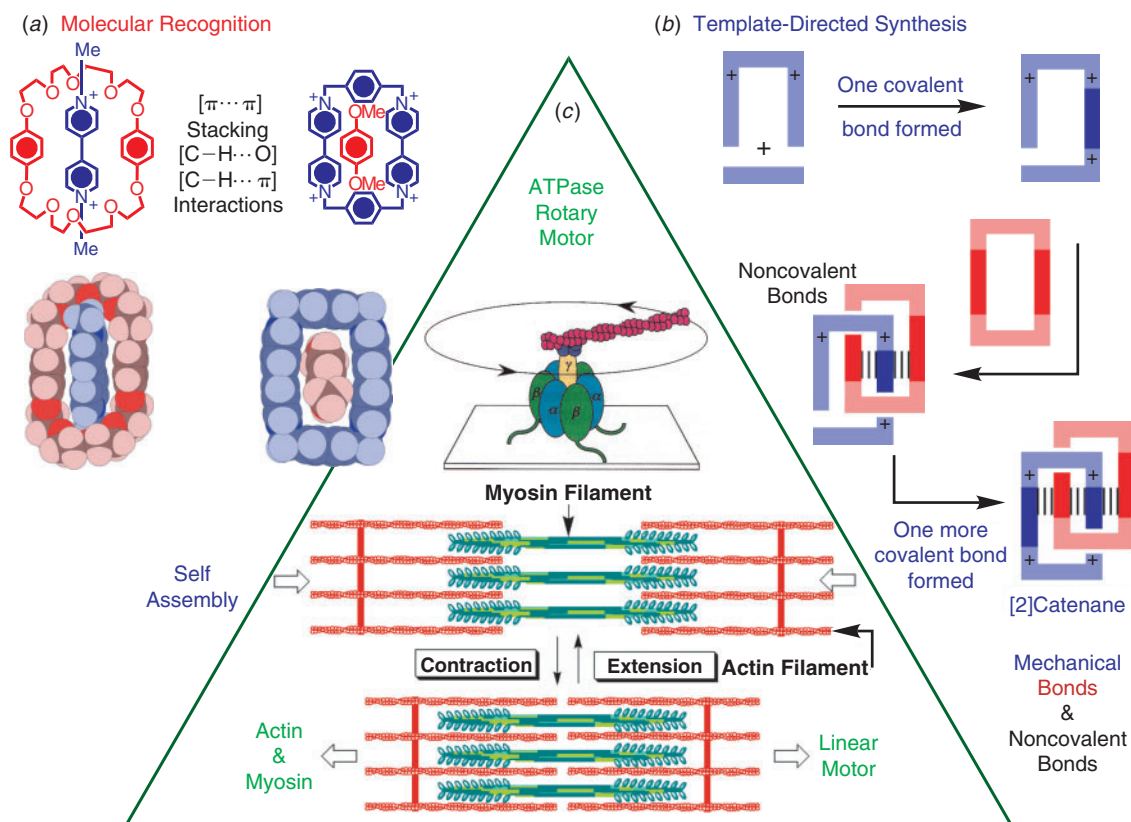


**Fig. 3.** Concept transfer from the life sciences into materials science has been the key element in the development of motor molecules. (a) Molecular recognition elements are used by natural systems to self-assemble pre-programmed molecular components spontaneously in a well-defined manner. Noncovalent bonding including  $(\pi \cdots \pi)$  stacking, together with  $(C-H \cdots O)$  and  $(C-H \cdots \pi)$  interactions, were incorporated into each aromatic host-guest pair to facilitate their self-assembly. (b) This system of mutually interacting molecular components was developed to aid and abet the formation of mechanical bonds employing template-directed synthesis. (c) The natural ATPase rotary motor and the actin-myosin linear motor provide biomolecular models. An understanding of their mode of operation will aid the design of wholly artificial motor molecules.

not only the solution switching behaviour of rotaxanes and catenanes,<sup>[38]</sup> but also their now proven facility to undergo switchable mechanical movements between two states within half-devices, a reasonable and wholly self-consistent nano-electromechanical mechanism for the switches operating in a solid-state electronic device will be proposed. From the ability to form large-area monolayers, the first crossbar device was made with bistable [2]catenane molecules integrated in between a Si bottom electrode and a Ti/Al top electrode. Success at this level spawned a top-down miniaturization thrust with the testing of a three-terminal single-molecule transistor, using a break junction operating at 4 K, and then onto a two-terminal switch, based on a single semiconducting carbon nanotube as the bottom electrode. These previous two investigations provided insight into the importance of selecting appropriate electrode materials. The data obtained from this survey of a range of molecular switches deployed in an array of full- and half-devices heralds the beginnings of a blueprint and guidebook for making and harnessing some of the world's tiniest machines. These first steps bring into focus the importance of considering every single element within a molecular electronics paradigm—the device's composition and architecture matter just as much as the molecules themselves.

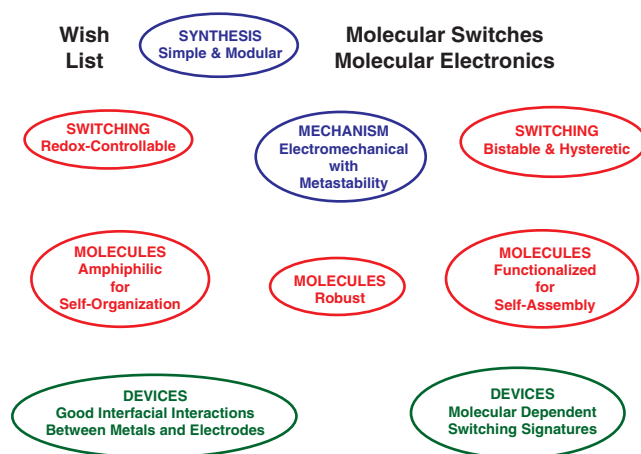


**Fig. 4.** Contemplating the design, preparation, and testing of electronic devices based on molecular switches requires a series of molecule and device properties that need to be satisfied.

The simple description of the crossbar device belies the inherently difficult challenges that were faced and overcome when a solution-phase system, which was well understood, was transferred onto a technology platform. At that stage, the wish list was long (Fig. 4). Fortunately, a rational approach

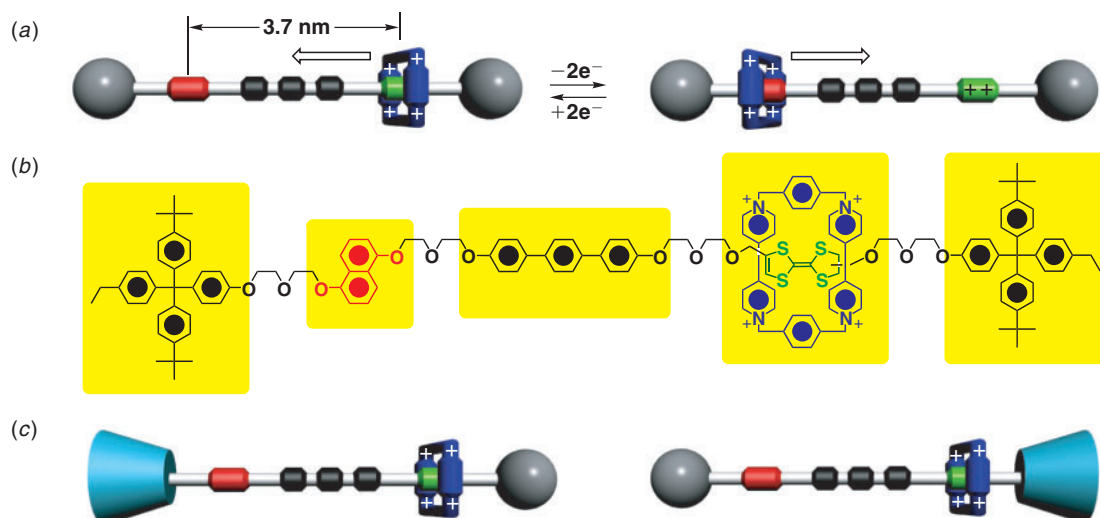


**Fig. 5.** A series of bistable [2]rotaxanes were prepared in order to satisfy and demonstrate some of the molecular elements required for the realization of a device incorporating molecules. (a) A graphical representation of a bistable [2]rotaxane that undergoes a redox-controllable 3.7 nm movement of the ring. (b) The structural formula of this rotaxane reveals its multicomponent nature. The rotaxane can be customized by modifying the modular synthetic procedure to install hydrophilic as well as hydrophobic stoppers. (c) Graphical representation of two variants of amphiphilic bistable [2]rotaxanes that are constitutionally isomeric.

toward meeting the challenges of molecular nanoelectronics can be broken down into simple stepwise modules. They are (a) the preparation of molecular switches and the demonstration of their mechanical operations (b) in solution, (c) in Langmuir–Blodgett (LB) monolayers, (d) in SAMs on gold, and ultimately (e) in solid-state devices.

### Mechanical Switching in Langmuir–Blodgett Half-Devices

In the rational progression toward a full electronic device, one step consists inevitably of the preparation and characterization of half of the device. For this purpose, Langmuir monolayers at the air/water interface and LB monolayers transferred to Si substrates have been investigated. Langmuir monolayers are formed from amphiphilic molecules that are capable of self-organization at an air/water interface.<sup>[39]</sup> A modular approach (Fig. 5), commonly used in the synthesis of multicomponent supramolecular systems, was employed effectively to adjust the lipophilicity<sup>[40]</sup> of rotaxanes. An amphiphilic, linear [2]rotaxane was prepared by replacing one of the hydrophilic tetraarylmethane head groups with a polyethylene glycol terminated one. In keeping with the modularity, the hydrophilic head group was swapped with the hydrophobic one at the other end, and a longer *p*-terphenyl spacer introduced between the TTF and DNP recognition sites along the dumbbell. The spacer was introduced in order to tune the shuttling barrier and to enhance rigidity. These two amphiphilic systems were found to form Langmuir monolayers readily at the air/water interface.<sup>[41]</sup> Prior to proceeding with the challenges associated with switching rotaxanes in compressed monolayers, it is important to demonstrate that these redesigned rotaxanes display the switching properties<sup>[38,42]</sup> that are expected of them in solution.

In these two-station [2]rotaxanes, both UV-visible and <sup>1</sup>H NMR (Fig. 6) spectroscopic data indicate that there is

only one translational isomer present in CD<sub>3</sub>CN at room temperature—in particular, the one with the CBPQT<sup>4+</sup> ring encircling the TTF unit exclusively in preference to the DNP ring system. These rotaxanes can be readily switched in solution using chemical redox agents and monitored using UV-visible and <sup>1</sup>H NMR spectroscopy.<sup>[43]</sup> With the *p*-terphenyl spacer, this switching results in a significant 3.7 nm movement.

Once these molecular machines had been demonstrated to work as expected in solution, they were transferred to—and constrained along two dimensions at—the air/water interface. Amphiphilic rotaxanes and their dumbbells were studied (Fig. 7) using Langmuir isotherm techniques in order to establish<sup>[44]</sup> their ability to form continuous monolayers and to assess their capacity to display switching in these types of condensed phases.

These, as yet unpublished experiments, establish beyond any shadow of a doubt that chemical oxidation of amphiphilic bistable rotaxanes in an LB-based half-device configuration causes the mechanical movement of the CBPQT<sup>4+</sup> ring. This result provides evidence for the operation of mechanical switching within half-devices that model the monolayer preparation of the full-devices. The balancing half is provided from a different half-device that incorporates an electronic stimulus for switching.

### Mechanical Switches Self-Assembled on Gold—The Other Half (Device)

Half-devices composed of switches self-assembled on gold electrode surfaces<sup>[36]</sup> provide considerable insight into full-devices, by placing a conceptual stepping-stone between molecules in solution and those sandwiched between two electrodes. In particular, a SAM of bistable [2]rotaxanes on gold electrodes<sup>[45]</sup> provides an inbuilt way not only to control electrochemically the operation of these nanoscale machines,

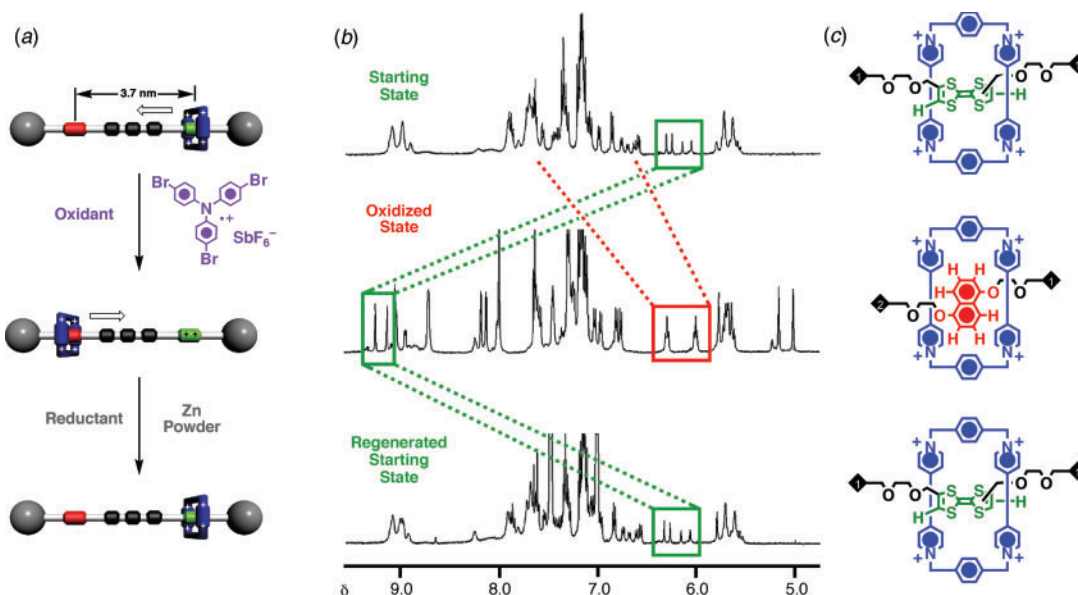


**Fig. 6.** (a) Representations of the amphiphilic bistable [2]rotaxanes, illustrating the oxidation state and ring location, after the addition of the oxidant, tris(*p*-bromophenyl)ammonium hexachloroantimonate, followed by the reductant, zinc powder. (b) The switching of the molecule is concomitant with changes in the  $^1\text{H}$  NMR spectra. (c) Both the shifts of the TTF- and DNP-based protons are consistent with the locations of the ring as illustrated.

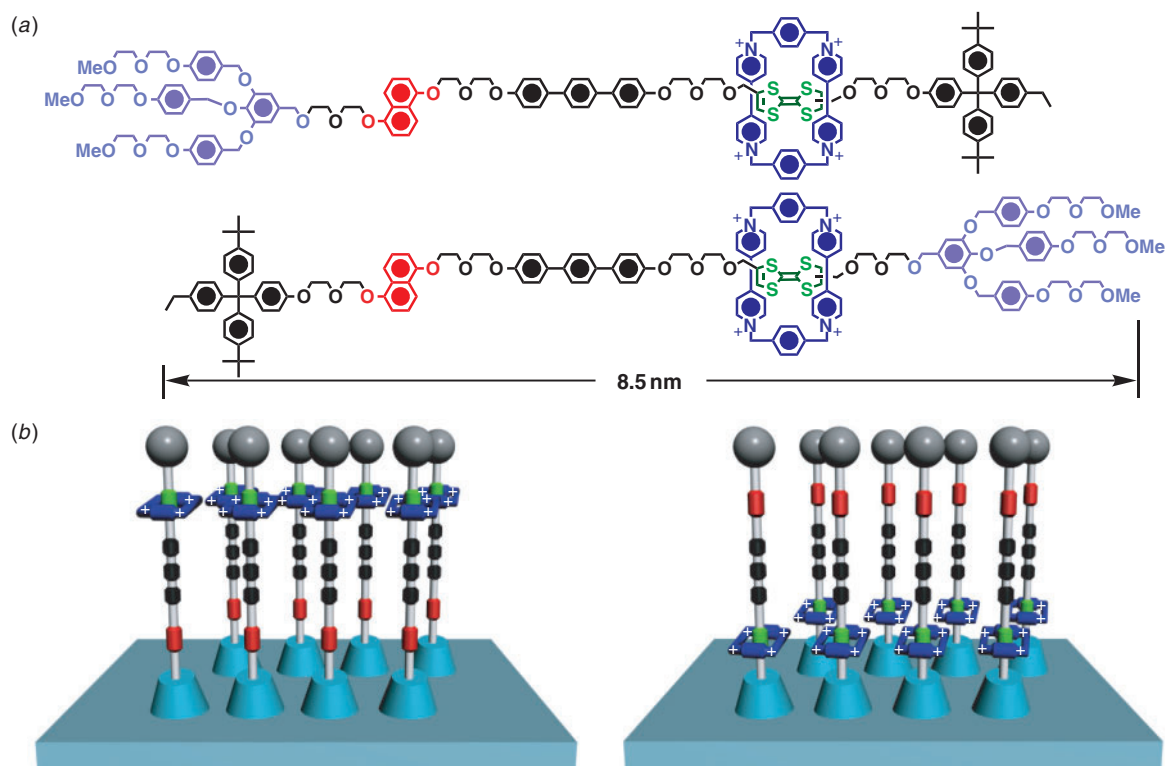


**Fig. 7.** (a) Structural formulas of the two amphiphilic bistable [2]rotaxanes that were designed to (b) self-organize at the air/water interface to form Langmuir monolayers. The *p*-terphenyl spacer was added to enhance the rigidity of the amphiphilic rotaxanes, and hence the stabilities of the monolayers, and also to control the shuttling of the ring between the TTF unit and DNP ring system. Note that the graphical representations of the isomeric [2]rotaxanes are highly idealized.

but also, through electrochemical experiments, to identify the mechanism of the switching process.

The modularity of the mechanically interlocked molecules was demonstrated again by the template-directed synthesis of

a bistable [2]rotaxane, wherein the head group adjacent to the DNP ring system is replaced with an isopropyl-based stopper, to which is appended a disulfide tether for self-assembly onto gold surfaces. Moreover, in this bistable rotaxane, the spacer

between the two recognition sites was shortened to a simple diethylene glycol chain.

Using a standard three-electrode cell adapted for temperature control, a series of CV experiments were conducted on the rotaxane and its dumbbell precursor. In a full reduction–oxidation cycle, the CV displayed a response that was consistent with the solution-phase electrochemistry.<sup>[42,46]</sup> That is, the reduction is localized on the ring and the oxidation on the TTF unit. The exact form of the CV displays splitting of the first ring-based reduction couple, which is consistent with the ring's involvement in noncovalent bonding with the TTF unit. Similarly, the TTF unit's first anodic oxidation peak is shifted, by comparison with the dumbbell compound, to more positive potentials, an observation that corroborates the encirclement of the TTF unit by the CBPQT<sup>4+</sup> ring. However, the second oxidation couple and the first oxidation's cathodic return peak are in similar positions to those of the dumbbell. These observations indicate that, once the TTF unit becomes singly oxidized, the ring no longer encircles it. Based on every other solution-phase electrochemical study, the ring moves to the DNP ring system, where it forms noncovalent bonds albeit of lower binding strengths than with the TTF unit. However, the bonds are sufficiently strong to slow down temporarily the ring's return to the TTF unit, once the system is returned to the neutral ground state.

Within this half-device configuration, the [2]rotaxane displays metastable as well as bistable behaviour. This characteristic is revealed (Fig. 8a) when a second oxidative cycle is performed. A new anodic peak is observed to grow concomitantly with a decrease in the intensity of the first anodic peak, observed in the initial cycle. By controlling the time between redox cycles and the temperature, a range of kinetic data were recorded, from which the activation energy for the ring's relaxation from the metastable state back to the ground state was established at 17.7 kcal mol<sup>-1</sup>. The lifetime of the metastable state could be extinguished by reducing the ring electrochemically. In this manner, any donor–acceptor interactions between the ring and the DNP ring system are switched off, allowing the ring to traverse the previously high activation barrier.

In summary, a complete nanoelectromechanical switching mechanism (Fig. 8b) has been identified for the SAM of rotaxanes on gold electrodes. Oxidation at +700 mV installs two positive charges on the TTF unit, creating charge–charge repulsion to drive the ring's mechanical movement to the DNP ring system. When the switching potential is removed, a metastable state is created and decays, in a thermally activated mechanical movement of the ring to the more favourable TTF donor with a high activation barrier. Alternatively, the ring's location can be reset by applying a potential of –600 mV, so returning the ring back to the TTF unit and the SAM of rotaxanes back to their ground state.

### Molecular Electronic Memory

The historical development of the molecular-based crossbar device did not follow logically from the half-devices but instead constituted a leap of faith from well-understood solution-phase switching<sup>[33,38]</sup> directly to the solid-state

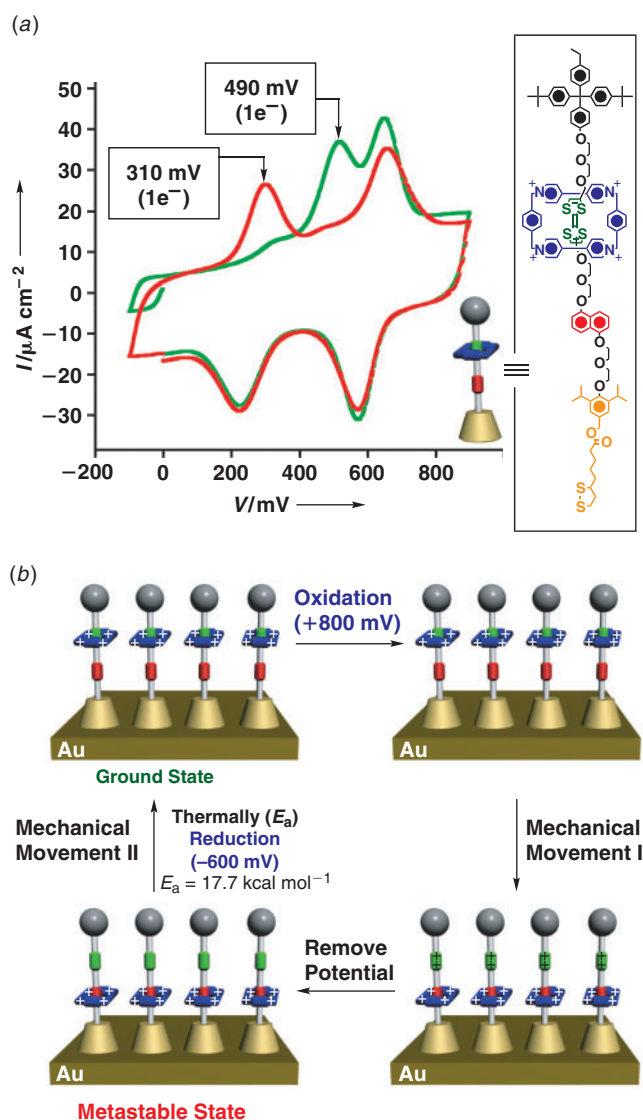


**Fig. 8.** (a) The first (green) and second (red) cyclic voltammograms ( $300 \text{ mV s}^{-1}$ , 288 K, 0.05 M LiClO<sub>4</sub>, MeCN) of a self-assembled monolayer of a disulfide-tethered [2]rotaxane (inset). The first cycle displays the expected response for a TTF unit that is encircled by the CBPQT<sup>4+</sup> ring ( $E_{a,p1}$  490 mV), whereas the second cycle displays the dumbbell-like response of a bare TTF unit ( $E_{a,p1}$  310 mV). (b) The proposed nanoelectromechanical mechanism for the operation of bistable [2]rotaxanes self-assembled onto a gold substrate under voltage control. In the ground state, the ring (blue) is located on the TTF unit (green) until a +630 mV voltage is applied. The TTF unit becomes doubly oxidized and charge repulsion drives the tetracationic ring in the first mechanical movement to the DNP ring system (red). When the voltage is removed, the TTF<sup>2+</sup> dication loses its positive charges, yet the ring remains weakly bound to the DNP ring system, forming a metastable state. The ring returns to the TTF unit by either a thermally activated process ( $E_a$  17.7 kcal mol<sup>-1</sup>) or, actively, by applying a negative voltage, of at least –600 mV to reduce the ring, thus releasing its grip on the DNP ring system allowing the ring to move more freely back to the TTF unit.

devices. The design requirements that needed to be fulfilled for the fabrication of a molecular junction are still as important now as they were then. In particular, for the linear rotaxanes, it is imperative to (a) build-in amphiphilicity to facilitate the deposition of smooth LB monolayers, and (b) for

the rotaxane to display chemically distinct and electronically addressable binding sites for the ring, namely bistability. In addition, it was necessary to (c) create enough ‘elbow room’ for the ring to be able to move easily up and down the dumbbell. The last requirement was satisfied by using stoppers at the head and tail of the rotaxane that were larger than the ring—a feature of these types of mechanically interlocked molecules that is coincidentally fulfilled by the constraints of the preparation and isolation of rotaxanes. With all of these criteria satisfied, devices were fabricated wherein the hypothesized mechanism for operation of the rotaxane-based switch follows on logically from the half-device. A positive bias oxidizes the molecule for a sufficiently long period of time for the mechanical movement of the ring to the DNP ring system to take place. When the bias is removed a metastable state is present, wherein the ring is located around the DNP ring system even though the repulsive charges on the TTF unit have been removed. The metastable state after about 15 min deactivates thermally back to the starting state, or it can be actively reset by applying a negative bias. In this manner, a hysteretic cycle is produced wherein the creation of the metastable state cannot be reset back to the ground state along the same pathway by which it was formed.

Although, generally speaking, the mechanistic steps for switching are comparable between half- and full-devices, the details differ. The lifetime (15 min) of the metastable state in full-devices is significantly longer than that (5 s) observed in half-devices. However, this observation is qualitatively consistent with the kinetics of shuttling in two-station degenerate [2]rotaxanes, revealed using  $^1\text{H}$ NMR spectroscopy,<sup>[47]</sup> that is, constriction in all directions in full-devices slows down the ring’s translocation significantly over the natural barrier to shuttling from the DNP to the TTF unit.

Finally, in full-devices, the threshold voltages for switching, which are assigned to the onset of oxidation and reduction redox processes, occur at +2 and –2 V, respectively, whereas in solution and half-devices these processes occur at +0.7 and –0.4 V, respectively. The large voltage shift is thought to reflect the differences between the two types of environments. On the one hand, Bocian and Lindsey<sup>[12]</sup> have verified that increasing the length of the tunnel barriers causes the redox potential for the onset of oxidation of a ferrocene compound self-assembled onto a silica surface to shift to more positive values. Furthermore, in a full-device once a redox process has occurred, there is an absence of additional counterions that are present in solution and half-device electrochemical studies to neutralize the charge imbalance arising from the formation of the charged redox state. Notwithstanding these apparent differences that originate, in our minds, from the nature of the boundary conditions imposed by the tightly packed monolayers and insulative silica layers in charge-balanced devices, the correspondence in bistability and metastability is remarkably close, consistent, and repeatable (see below).

The two types of half-devices investigated—namely (a) amphiphilic bistable rotaxanes closely packed on silicon substrates and (b) electrode-bound, electrochemically stimulated bistable rotaxanes with demonstrable metastability—both demonstrate that mechanical switching of the CBPQT<sup>4+</sup>

ring along the dumbbell component can occur in either environment. Insofar as these two halves constitute conceptually most of the whole, their behaviour forms a basis to rationalize the memory devices built around molecular switches, sandwiched between two electrodes.

#### *Constructing a Molecular Switch Tunnel Junction (MSTJ)*

From a molecular perspective, the crossbar devices are made (Fig. 9) in an ordered fashion by the self-organization of amphiphilic rotaxanes into stable Langmuir monolayers, which are then transferred to a silicon electrode as an LB monolayer. The silicon electrode is highly doped so as to make it as conductive as possible. In addition, a native oxide,  $\text{SiO}_2$ , is allowed to grow, thus making the electrode’s preparation simple by avoiding the complex procedures required for clean-room quality fabrication. The entire sandwich is completed by the deposition of a molecule-friendly titanium capping-layer and finished off with an aluminium electrode. When the junction is prepared on silicon nanowires of 70 nm width, and when the top electrodes are lithographically defined to be 100 nm in width, the number of molecules trapped in the crossbar device between the two electrodes is of the order of 5000. In this manner, a crossbar device with a molecular switch defines a tunnel junction.

The writing and reading of an MSTJ device is determined ultimately by the nature of the molecule and, in particular, by its nanoelectromechanical switching mechanism. The device can be interrogated using a customized ‘writing voltage and reading current’ protocol. The write voltage is a variable, which, when preset, is sent to the crossbar for a limited duration and then returned to the reading voltage of +100 mV. The current flowing through the device is read out through a preamplifier to ground when the voltage is held at +100 mV.

For the purposes of device characterization (Fig. 9b), a remnant molecular signature, akin to recording magnetization hysteresis,<sup>[48]</sup> is recorded. These signatures are generated when the voltage component of the write–read protocol is cycled in 40 mV steps from 0.0 V, up to +2 V, down to –2 V, and back to 0.0 V. In this manner, the threshold voltages for switching the device between low and high conductance states can be measured experimentally. In almost all cases, the qualitative remnant molecular signatures obtained from a range of catenanes and rotaxanes are similar. The device is maintained in a low conductance state until the write voltage reaches +2 V. At this point, reading the device at +100 mV will reveal the presence of the higher conductance state. The device persists in this state until the write voltage reaches another threshold at –2 V. Here, the current that is read out at +100 mV has returned to a lower conductance state, where it remains while the writing voltage is stepped back to 0.0 V. The hysteresis in the remnant molecular signature is recorded only for those devices that are made from switchable molecules. When control amphiphilic molecules, such as the free dumbbell compound or eicosanoic acid are used to prepare the devices, no hysteresis is observed.

The device’s switching between low (0, OFF) and high (1, ON) conductance states displays a binary character

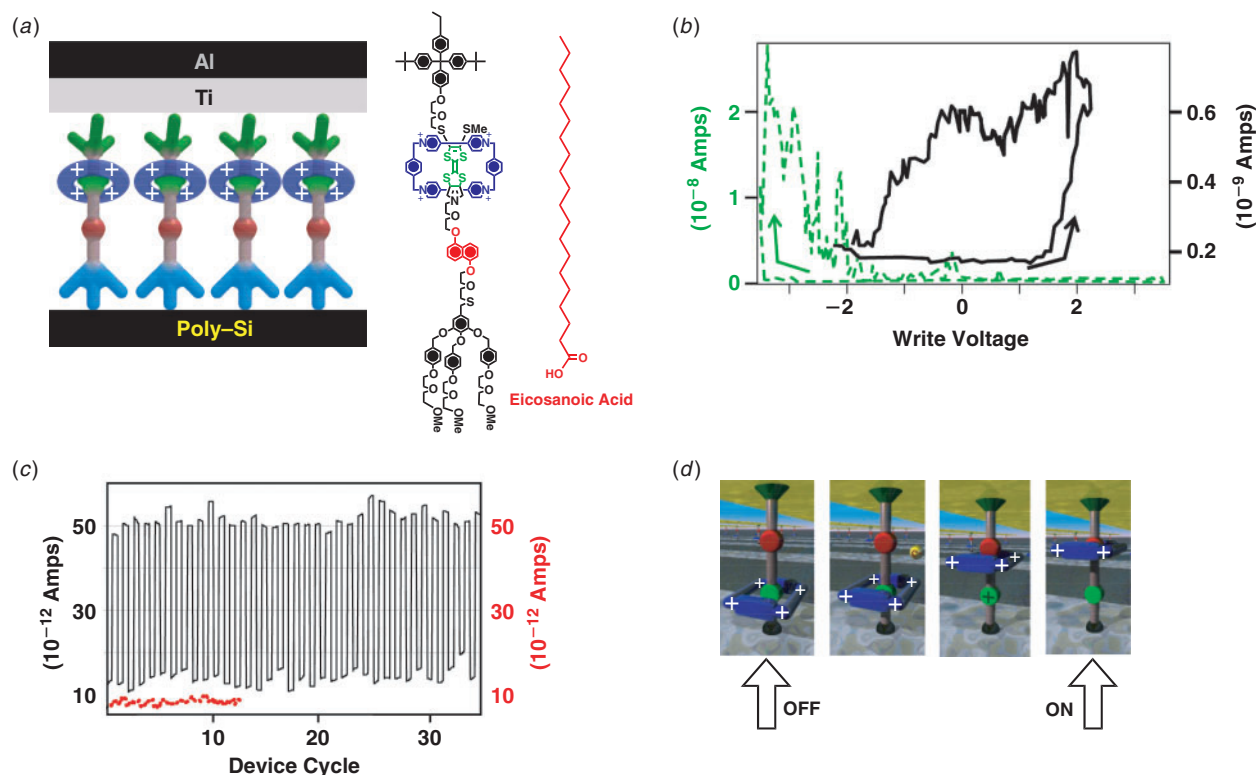


**Fig. 9.** MSTJ devices have been constructed and tested in which a monolayer of closely packed amphiphilic bistable [2]rotaxanes are sandwiched between a Si bottom electrode and a Ti/Al top electrode. (a) Structural formula of an amphiphilic bistable [2]rotaxane and the non-redox active control compound, eicosanoic acid, together with the graphical representation of a device. (b) The remnant molecular signature of a micrometer-scale MSTJ device, and (c) the binary device characteristics of a nanometer-scale device. Both of the devices incorporate the amphiphilic bistable [2]rotaxane. The micrometer-scale device is compared to the dumbbell-only (green) counterpart and the nanometer-scale device to eicosanoic acid (red). The remnant molecular signature displays the measured current (y-axis) flowing across the junction recorded with an applied voltage of +100 mV against a series of voltage pulses (x-axis) stepped at 40 mV intervals that map out the hysteresis loop. A record of the remnant molecular signature allows the threshold voltages to be identified and then used to define the switching voltages used for (c) the demonstration of binary memory storage. Each cycle in the binary memory trace represents closing (+2 V) and opening (−2 V) the switch with the current read out with +100 mV applied across the device. The trace illustrates 35 cycles of writing, reading, erasing, and reading the device. (d) Graphical representations of the switching mechanism, illustrating the location of the ring for the OFF and ON state.

(Fig. 9c) when the write–read protocol is appropriately customized. To write a 1 or a 0, a +2 or −2 V signal is applied to the bottom silicon electrode, respectively. The results indicate that this binary switching can be repeated more than 30 times with ON/OFF ratios of two to three for bistable catenanes and approximately ten for bistable rotaxanes. The same experiment, when it is conducted on devices made from eicosanoic acid, do not display any difference in current flow from cycle to cycle. Moreover, the ON states are observed to relax thermally to the OFF state in a manner qualitatively similar to the behaviour observed<sup>[45]</sup> in the half-devices based on SAMs of bistable rotaxanes on gold electrodes. These results, which were obtained from interrogation of the MSTJ devices, while phenomenological in nature, are, in every aspect, in qualitative agreement with the nanoelectromechanical switching observed in solution and in the LB and SAM half-devices. Consequently, the device's switching is assigned to a molecular property and the same switching mechanism, as that outlined for the half-devices, is proposed to account for the observed phenomena—albeit with slightly different magnitudes for the switching voltages.

#### Proposed Nanoelectromechanical Switching Mechanism

A molecule-based nanoelectromechanical switching mechanism, which is consistent with all the data obtained to date, has been proposed (Fig. 10) to account for the device's observed behaviour. In the device, application of a +2 V bias to the Si electrode generates an oxidized form of the sandwiched rotaxane—either the mono or dicationic form of the TTF unit. Based on the number of molecules in each junction and by counting the number of electrons passed across the device at +2 V, only one in every hundred electrons participates in the formation of the oxidized state.<sup>[8b]</sup> Just as in solution, the resulting repulsive force is predicted to drive the ring away in a mechanical movement, such that it localizes itself around the DNP ring system. When the bias is lowered to +100 mV for the purposes of reading the device, the charge on the TTF unit is believed to be neutralized. However, the CBPQT<sup>4+</sup> ring remains localized at the DNP ring system on account of the combination of attractive noncovalent interactions and steric barriers to shuttling. Once in this high conductance state, the device is observed to decay in a manner that is qualitatively similar to that of the half-device. Thus, the decay rate is concomitant with the thermal relaxation of the ring back to the

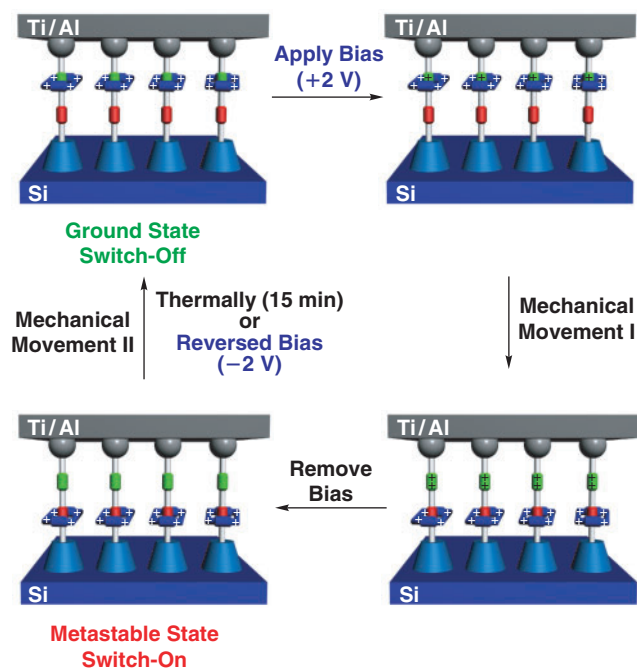


**Fig. 10.** Graphical representation of the proposed nanoelectromechanical mechanism outlining the concomitant oxidation states and idealized location of the ring in bistable [2]rotaxane molecules in an MSTJ device. Starting from the ground state—switch-OFF configuration—a bias of +2 V applied to the Si bottom electrode with the Ti/Al grounded is a sufficient driving force to oxidize the TTF unit for a long enough period of time to drive the mechanical movement of the ring to the DNP ring system. Lowering of the bias to +100 mV for reading the current neutralizes the TTF unit. The resulting metastable state corresponds to the switch-ON state, which relaxes thermally after about 15 min at room temperature. Alternatively, the active switching to the OFF state can be achieved by an applied bias of -2 V, effectively resetting the location of the ring back to the TTF unit.

thermodynamically more favoured TTF unit. Alternatively, the ring can be switched back by applying a reverse bias of -2 V, which results in the reduction of the ring, leading to its second mechanical movement back to the TTF unit.

It has been observed that the barrier to thermal relaxation increases from  $14.5 \text{ kcal mol}^{-1}$  in solution<sup>[47]</sup> to a situation where a certain degree of confinement in a SAM<sup>[45]</sup> produces a  $17.7 \text{ kcal mol}^{-1}$  barrier, corresponding to a lifetime of 5 s at 293 K. When the level of confinement is along all three dimensions in an MSTJ device, the lifetime is extended to 15 min at a similar temperature.<sup>[8]</sup> The qualitative observation of thermally activated behaviour in all three situations is one of the key correlations, together with the control experiments performed on molecules that do not switch, that provide the most compelling experimental indication of the molecule's involvement in the observed device switching. The proposed mechanism of switching assigns the low conductance state (OFF) to that with the ring encircling the TTF unit. It follows, therefore, that the ON state, which is metastable in character, is assigned to the situation where the ring is located around the DNP ring system.

The physical basis behind the changes in the measured conductance at +0.1 V between the ON and OFF states is still a matter of investigation. Nevertheless, if

the nanoelectromechanical cycle of the switching is occurring as proposed, then the changes in conductance may be attributed in part at least to the switching of the TTF-based molecular energy levels into and out of resonance with electron tunnelling pathways at the energies set by the reading voltages—or, put another way, the ON and OFF states correspond to the situation where the energy difference between the rotaxane's highest occupied and lowest unoccupied molecular orbitals (HOMO, LUMO) is smaller and larger, respectively. This hypothesis has been tested (Fig. 11) by means of first-principles computation. In these studies, the current  $I$  was calculated as a function of voltage  $V$  by simulating a metal–molecule–metal device. The physical model relies on a simplified version of a switchable [2]rotaxane, connected at either end to gold electrodes, which were modelled as a cluster of three gold atoms each. The structures of the molecule and the electrodes were computed from first principles to obtain the transmission function<sup>[49]</sup>—a measure of the degree of electron transmission between the two electrodes through the potential energy landscape defined by the molecule. The  $I$ - $V$  characteristics were calculated for the proposed ground and metastable states of the molecule. A higher conductance, assigned to the ON state, was computed for the molecular structure (metastable state) where the ring is located around the DNP ring system, whereas in the calculated low conductance, or OFF, state the ring is localized around the TTF unit in the molecular structure (ground state). The results obtained are strikingly consistent with the proposed switching mechanism. In principle, the difference in the computed conductance levels should be reflected in the underlying electronic structure of the two forms of the rotaxanes.

From the first-principles simulation, the molecular orbital (MO) energies for the two states of the molecule were generated. On going from the OFF state to the ON state, the HOMO energy displayed the largest shift of about 1 eV to higher energies, making it possible for it to lie closer to the Fermi levels of the electrodes. This difference in position of the energy levels is consistent with the notion that the switching of the molecule-based resonant tunnelling pathways contributes to the devices' switching characteristics. In such a simplified calculation, the effect of the contribution of the tunnel barrier by both the  $\text{SiO}_2$  and the rotaxane's bulky stoppers in the real devices has not been evaluated. To the best of our knowledge, the actual electrical conduction mechanism is likely to be a combination of hopping and tunnelling.<sup>[50]</sup> Nevertheless, the 1 eV shift is quite dramatic. The correlation of the lower HOMO energy for the OFF state associated with the CBPQT<sup>4+</sup> ring encircling the TTF unit and then the HOMO's movement to higher energies for the ON state, for the case where the CBPQT<sup>4+</sup> ring encircles the DNP ring system, matches qualitatively with the electrochemical data for bistable [2]rotaxanes in solution<sup>[46]</sup> and in half-devices.<sup>[45]</sup> In these cases, the HOMO energy may be approximated by the oxidation peak potential.<sup>[51]</sup> Here, the oxidation potential shifts from +0.7 V (versus SCE) in the case where the CBPQT<sup>4+</sup> ring encircles the TTF unit—the translational isomer assigned to the OFF state—down to

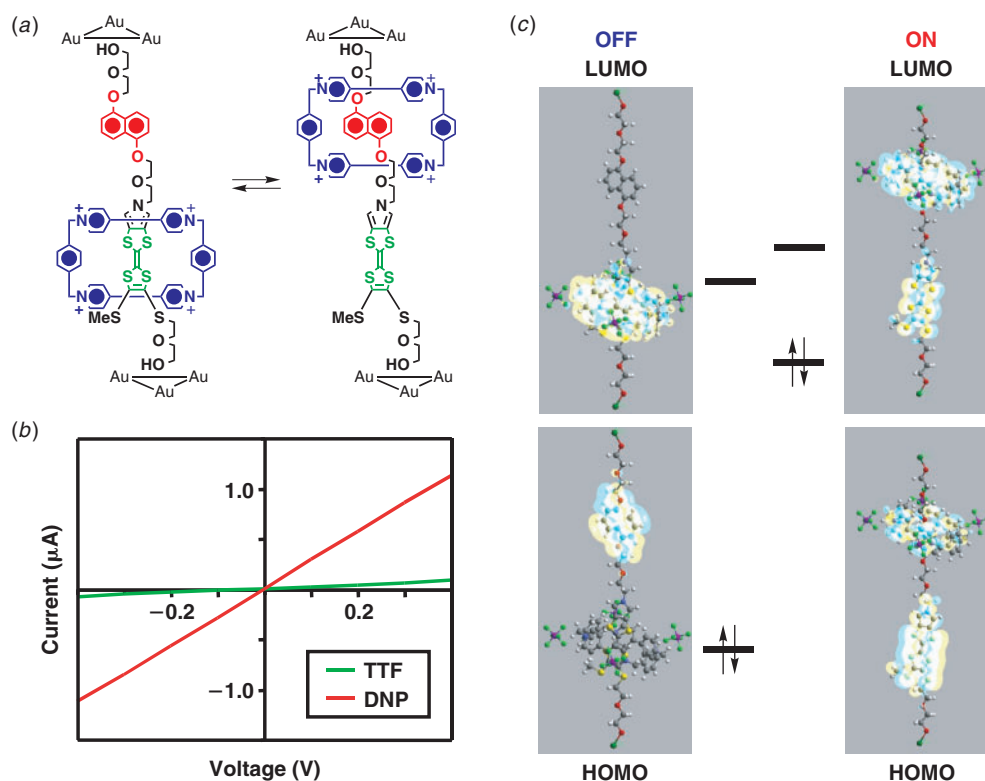


**Fig. 11.** (a) Structural formulas of the two metal-molecule-metal models used to simulate computationally the MSTJ device from first principles. The molecules had their stoppers removed and the electrodes replaced by a cluster of three gold atoms in order to simplify the calculation. (b) The calculated  $I$ - $V$  curves for each state of the molecular switches. These results show clearly that the translational isomer with the ring located around the DNP ring system is more conducting than the other isomer. (c) The energies and graphical representation of the HOMOs and LUMOs for each state. In the ON state, the HOMO and LUMO are delocalized to a certain extent and the energy of the HOMO is shifted dramatically.

+0.45 V (versus SCE) for the bare TTF unit corresponding to the ON state, a total shift in the same direction as that calculated but of only 0.35 V. In summary, the results obtained from these quantum chemical experiments not only adds credence to the hypothesis that resonant tunnelling contributes to electrical transport but also further supports the assignments of the rotaxane's translational isomers that correspond to the observed ON and OFF states of the electronic devices.

### Memory Devices

A simple crossbar provides the basic element from which to construct a memory device. A  $6 \times 6$  crosspoint structure comprised in total by 36 MSTJs containing a monolayer of amphiphilic bistable [2]rotaxanes was constructed. Of the total number, only 25 crosspoints, or bits, were operational and 16 of them were selected for a demonstration of the memory circuit's performance. The writing and reading of these devices follows the same protocols as those established for the single crossbars with one modification. In order to write to just one crosspoint, one of the leads is set to +1 V and the other -1 V, thus defining +2 V at the address of interest. With all the other leads grounded, only +1 or -1 V is felt at all the other non-addressed crosspoints. This procedure allows selective addressing. In these systems, a switch ON reads in the region of 75–200 pA of current, whereas the OFF state

reads out only 2–5 pA. In this way 16-bit RAM was demonstrated and provides a proof-of-principle demonstration of molecular random access memory (RAM).

The number of crosspoints was increased in order to demonstrate (Fig. 12) a 64-bit molecular RAM chip. Although damage along one of the  $8 \times 8$  wires led to a situation with only 56 bits in operation, the acronyms DARPA, SRC, and CNSI were successfully written and read as ASCII code. Contrary to standard RAM, where the memory addresses need to be continually rewritten every tens of milliseconds, these molecular analogues hold their switched ON state with a half-life of the order of 15–60 min. The ability to construct memory chips reliably from molecular switches bodes well for future applications. Furthermore, the close correlation between the behaviour observed in solution, half-devices, and full-devices, as well as the quantum chemical simulations of the full-devices, lends credence to the proposed nanoelectromechanical mechanism of switching. Ultimately, this understanding may serve as an appropriate basis from which to optimize the memory chip's performance.

### Three-Terminal Single-Molecule Devices

In an effort to produce a single-molecule transistor, a break-junction device using platinum electrodes, coupled with a third Si/SiO<sub>2</sub> gate electrode, was fabricated.<sup>[52]</sup> These devices

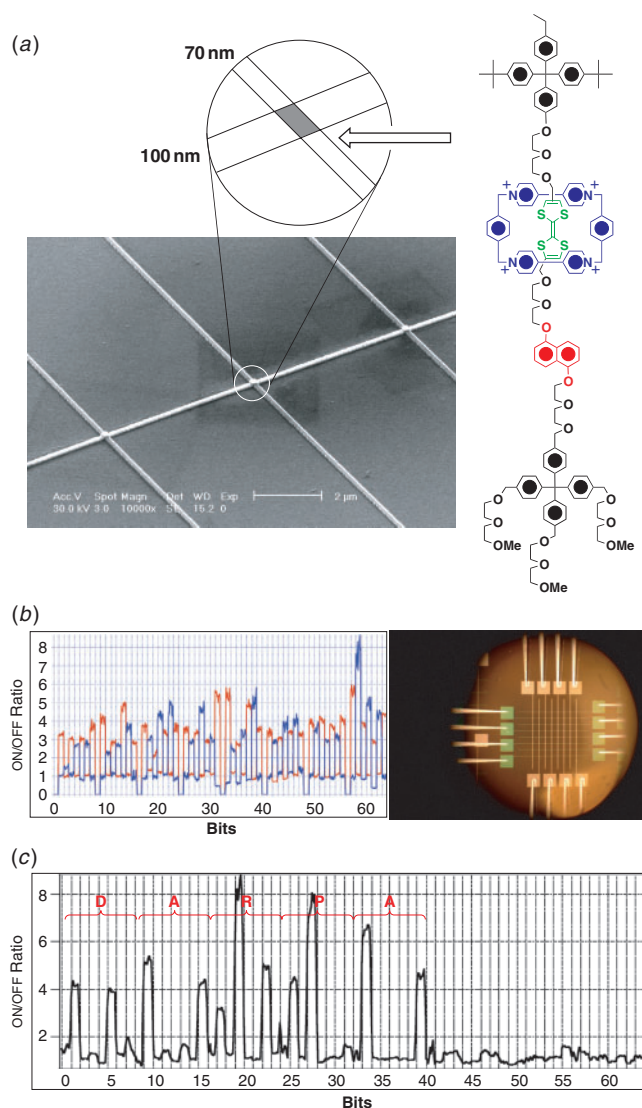


**Fig. 12.** (a) Telescopic representation outlining the location of  $\sim 5000$  bistable [2]rotaxane molecules at a crosspoint of a 1D circuit of MSTJs (SEM image). (b) An  $8 \times 8$  grid (inset) of crosspoint MSTJs was used to produce 64 bits of memory. The ON/OFF ratio of each bit was measured to identify their performance. These data reveal that only 56 of the 64 bits were operational. One wire, for whatever reason, malfunctioned. (c) The memory was used to write to and read out the word DARPA from the device in ASCII code.

allow the electrical transport through a single molecule to be recorded between two electrodes as a function of the applied bias and gate voltage.<sup>[53]</sup> In principle, rotaxane-based molecular systems could behave as a structurally flexible quantum dot, resulting in a resonant tunnelling transistor-type device. The asymmetric location of the TTF–CBPQT<sup>4+</sup> unit and the DNP ring system along the molecule's length would be predicted to confer an asymmetry to the observed differential conductance measurements.

Two types of rotaxanes were prepared for these measurements in order to bridge across the break junction. The first bistable [2]rotaxane (see Fig. 8) displays at one end of the dumbbell component a tetraaryl stopper for physisorption and at the other a disulfide for chemisorption to the platinum

electrodes. The differential conductance measurements recorded at 4 K displayed an asymmetric differential conductance signature as predicted. However, the simple observation of the asymmetry was tested in a control experiment that utilizes a rotaxane, which instead carries symmetric, chemisorbed, disulfide-based end groups. This molecular control displayed a symmetric differential conductance signature irrespective of the asymmetry in the location of the TTF–CBPQT<sup>4+</sup> and DNP units. Consequently, this result suggests that, in these types of break-junction devices, the electronic states of the DNP ring system and those of the TTF unit complexed with the CBPQT<sup>4+</sup> ring are overshadowed by the surface states governing the interface between the molecule and the electrodes.<sup>[54]</sup> Such a finding appears superficially to be inconsistent with the importance of the molecular states in the silicon-based crossbar devices. However, we suggest that this result highlights how the device, now in its entirety, should be examined holistically for its ability to reveal molecule-based phenomena.

### Molecular Switch Tunnel Junction Based on a Carbon Nanotube

#### A Device Based on a Bistable [2]Catenane

The simple inclusion of any molecular switch into a crossbar device relies upon their deposition as a condensed monolayer. Whereas the rotaxanes could be customized to display amphiphilic character for facile Langmuir monolayer formation, the basic catenane structure consisting of two mechanically interlocked rings precludes this type of maneuvering. Consequently, the anionic cosurfactant derived from dimyristoylphosphatidic acid (DMPA) was an essential complement to the aqueous solubility of bistable catenanes conferred by its high ionic character.<sup>[44,55]</sup>

The Langmuir monolayers of bistable catenanes were characterized as an isotherm<sup>[44]</sup> and the logical extension was to rinse and repeat with the addition of the oxidant  $\text{Fe}(\text{ClO}_4)_3$  dissolved into the subphase. The isotherms were distinctly different and an analysis of the data revealed that, upon oxidation, the catenanes that now contain six positive charges had acquired two additional  $\text{DMPA}^-$  anions as a natural balance. Upon compression on the Langmuir trough, these assemblies of hexacationic catenanes and six  $\text{DMPA}^-$  anions are believed to self-organize into an alternating pattern, until a transition region is traversed along the isotherm where the area per molecule halves approximately to  $150 \text{ \AA}^2$ . At this point the  $\text{DMPA}^-$  anions are more than likely to be closely packed in a layer sitting above a layer of catenanes. Monolayers of the unswitched and switched catenanes were further characterized by scanning-tunnelling spectroscopy after their transfer onto Au(111), using the horizontal lifting technique at pressures below the onset of the Langmuir monolayer's transition region. The  $I$ – $V$  curves of the two forms differ, to the extent that higher conduction was displayed by the hexacationic system. The simple preparation of high-quality LB monolayers of a catenane molecular switch was a key result for the realistic inclusion of a differently shaped molecular switch in a MSTJ.

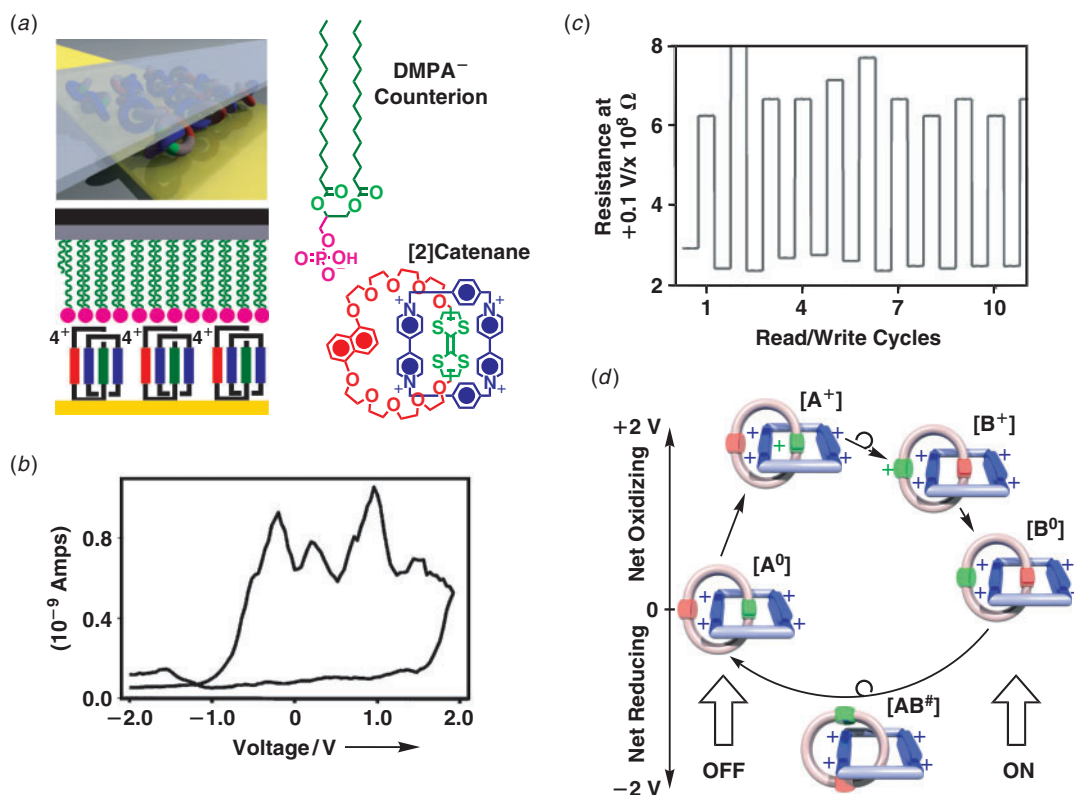


**Fig. 13.** Illustration of the [2]catenane-based MSTJ devices for comparison to the devices incorporating bistable [2]rotaxanes outlined in Figure 9. (a) The bistable [2]catenane is similarly constituted by the same tetracationic ring and the TTF unit and DNP ring system. The monolayers differ, in that, for the catenane, there is an additional layer contributed by the DMPA<sup>-</sup> anion. (b) The remnant molecular signatures are similar in their shapes, and switch-ON voltages (+2 V), but different in their switch-OFF voltages, namely -1 and -2 V, respectively, and in their ON/OFF ratios of about three and ten, respectively, for [2]catenane- and [2]rotaxane-based devices. (c) The binary switching behaviour is strikingly similar. (d) The proposed nanoelectromechanical switching mechanism differs only in that the [2]catenane undergoes a circumrotation, rather than a linear, mechanical motion.

MSTJ devices constructed from [2]catenanes display (Fig. 13) qualitatively the same features as those of the [2]rotaxanes (compare Fig. 9). The remnant molecular signature displays switching on at +2 V and switching off at -1 V, with ON/OFF ratios of about two to three observed from the binary switching experiments.<sup>[7]</sup> The nanoelectromechanical cycling of the catenane within the device is proposed to operate in a similar fashion to that of the rotaxanes, with the exception that it is a circumrotational motion, rather than a linear one. That is, the OFF state corresponds to the co-conformer with the TTF unit inside the ring. A +2 V write bias across the junction is proposed to cause a circumrotational process, thus positioning the DNP ring system inside the ring. A -2 V write bias returns the system to the OFF state, thus completing a full cycle. Just as in the rotaxane cases, the circumrotational processes are voltage-activated and the ON state is the metastable one with an associated thermally activated relaxation back to the OFF state.

The general method for fabricating devices around catenanes and rotaxane are remarkably similar. Starting from a smooth silicon substrate, thin parallel polycrystalline silicon (*p*-Si) electrodes were photolithographically patterned onto the surface. Following the preparation of the bottom *p*-Si electrode, the LB monolayer of either bistable [2]catenanes or bistable [2]rotaxanes are transferred to the substrate. The

Ti top electrode is vapour-deposited through a mask on top of the monolayer at an angle orthogonal to the underlying Si electrode. For the [2]catenane, it is the DMPA<sup>-</sup> counterions that protect the electroactive molecule. However, in the case of the rotaxanes, their hydrophobic tetraarylmethane head groups are sufficiently closely packed to prevent penetration of the hot titanium into the electroactive layer or to the bottom electrode. Subsequently, the device's remnant molecular signatures are recorded. The remnant molecular signatures of the bistable catenanes and rotaxanes are almost identical, except for the -1 V required to reset the switch OFF for the catenanes compared with the -2 V for the rotaxanes. The devices' suitability for memory applications were tested using ON/OFF write-read cycles. Again, there is little difference between the two molecular switches. The importance of the switchable molecules on device performance is tested through the use of degenerate control molecules. Again the results are the same—the control devices do not display hysteretic remnant molecular signatures and neither do they display binary switching behaviour.

#### *A Molecular Switch Tunnel Junction Based on a Carbon Nanotube*

The ultimate and inevitable evolution of molecular electronics finds its expression in a device defined by a

single molecule that switches the conduction between two nanowires. For attachment to silicon or metal nanowires, derivitization with hydroxyl<sup>[13]</sup> or disulfide-terminated rotaxanes may be possible. For attachment<sup>[56]</sup> to carbon nanotubes (CNTs), a pyrene-based rotaxane was initially investigated with no success. The absence of self-organization of the rotaxanes on the CNT caused shorting of the devices.

Consequently, the cationically charged analogue to pyrene, the diazapyrenium (DAP<sup>2+</sup>) unit,<sup>[57]</sup> provided rapid access (Fig. 14) to a bistable [2]catenane which, when spread onto a water surface using DMPA<sup>-</sup> as the counterion, formed stable Langmuir monolayers. Devices were fabricated<sup>[9]</sup> on the nanoscale using a modification of the general method developed for the bistable catenane devices first developed using a Si bottom electrode. In this case, the semiconducting CNTs that were spun onto an insulating SiO<sub>2</sub> substrate were identified and wired for electrical connectivity. LB monolayers of the DAP<sup>4+</sup>-based catenane were transferred, again topped with a monolayer of DMPA<sup>-</sup> counterions for protection from the Ti/Al top electrodes. It is considered more than likely that the outside diazapyrenium unit of the tetracationic macrocycle forms a  $\pi$ - $\pi$  interaction with the CNT.

In analogy with the control studies undertaken (Fig. 15) on the bistable rotaxane devices, two additional controls of the bistable DAP<sup>4+</sup>-based catenane were conducted. One control compound uses just the free DAP<sup>4+</sup> ring with no interlocking counterpart. Another retains the interlocking rings motif of the catenane, but utilizes a crown ether macrocycle—namely BPP34C10—with two identical  $\pi$ -donors and so does not possess any switchable character. The remnant molecular signatures of these three systems are revealing. Only the bistable catenane displays a hysteretic signature, resembling that of all the other switchable devices. A minor shift in the writing voltages to  $\pm 2.5$  V was required to guarantee binary switching activity. The same write-read cycles applied to the degenerate catenane produced no changes in the current, effectively displaying a flat line.

This series of measurements highlight the relative importance of the molecules in determining the device's switching properties, at the expense of the electrode/molecule interface. The success using *p*-Si and CNTs as one of the electrode contacts, together with the failure<sup>[52]</sup> of the single-molecule break junction devices in contact with platinum, defines an empirical result that has so far emerged from this molecular electronics research program. That is, the choice of the contact electrode material is important for directing the device's behaviour. This is no accident. The nature of the electrode material defines to a large extent the character of the molecule/metal interface.<sup>[45]</sup> In the cases where the electronegativity of the two materials do not match closely, charge transfer and other factors may lead to interfacial barriers for electron transport, akin to the Schottky barriers present in heterojunctions. In these cases, the molecule/metal interface is no longer 'transparent' and the electronic signature of the molecule may become partially or wholly masked. It follows from this reasoning that molecular interfaces with silicon and carbon electrodes will be favoured for the construction of devices intended to reveal molecular switching

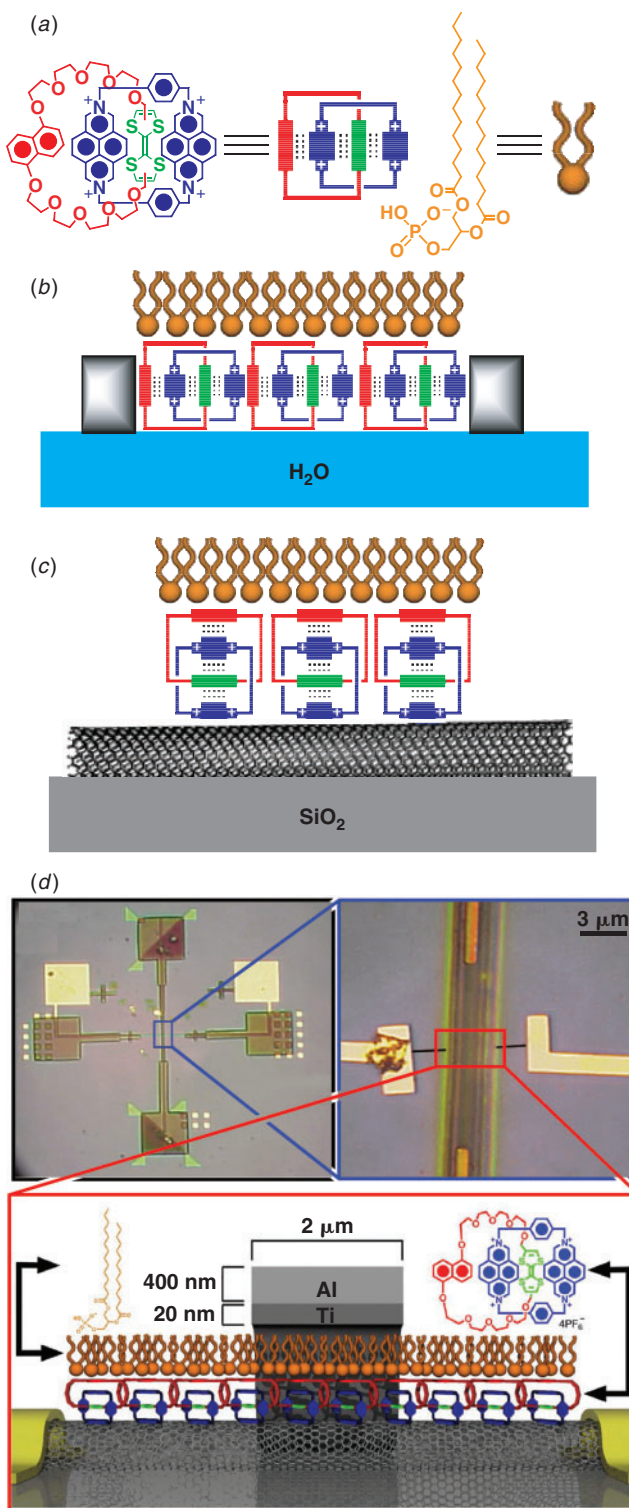


**Fig. 14.** (a) Structural formulas and graphical representations of the DAP<sup>4+</sup>-based [2]catenane and the DMPA<sup>-</sup> anions. (b) Graphical representations of the DAP<sup>4+</sup>-based catenane and the amphiphilic DMPA<sup>-</sup> counterions self-organized in a Langmuir monolayer at the air/water interface, before being transferred to (c) a semiconducting CNT on a SiO<sub>2</sub> substrate. (d) Telescopic representation illustrating how the crosspoint is wired from the outside world with electrode pads, in which the horizontal pair connect to a single nanotube (artificially colored black) that is crossed following monolayer deposition by the 2 μm wide Ti/Al top electrode. The final telescopic view is a graphical representation of the MSTJ, illustrating the crosspoint's constitution (not to scale).

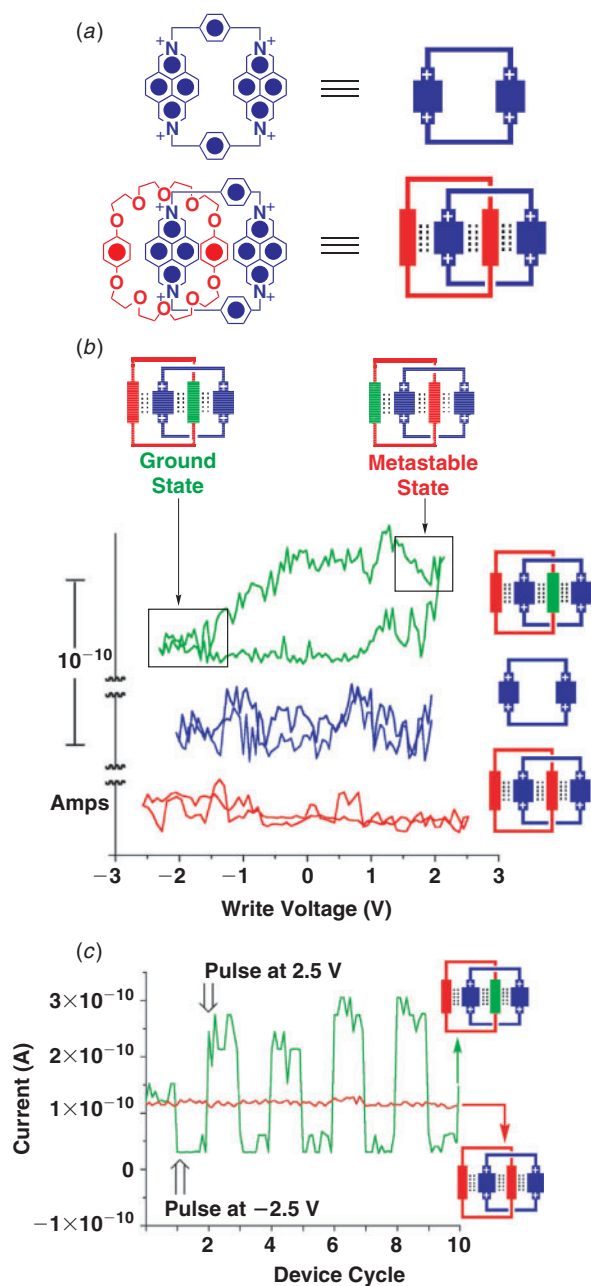


**Fig. 15.** (a) Structural formulas and graphical representations of the control molecules in the form of a single tetracationic DAP<sup>4+</sup> ring and a degenerate [2]catenane. (b) The remnant molecular signature for the bistable [2]catenane displays hysteresis, whereas the two controls do not. (c) The MSTJ, fabricated from the bistable [2]catenane, displays switching between high and low currents with an ON/OFF ratio of approximately eight, whereas the degenerate control [2]catenane displays a single flat line under identical conditions.

from the classes of bistable catenanes and rotaxanes discussed in this review.

A caveat to this rationalization is that different classes of compounds might function perfectly well as molecular switches when metal electrodes only are used. For example, SAMs of simple aromatic compounds with thiol end groups for attachment to gold electrodes have been shown to display<sup>[21]</sup> negative differential resistance (NDR), a phenomenon which has also been attributed to a molecular

property. By contrast, these  $\pi$ -systems have a highly conjugated backbone from which the mode of conduction, and thus the electrical transport behaviour, may differ substantially from that occurring in catenane- or rotaxane-based devices.

Now that an empirical hypothesis has been advanced for the classes of bistable molecular switches discussed in this review, it is scientifically informative to point out the differences (Table 1) between results obtained when both the top and bottom electrodes are metallic. Specifically, devices fabricated with a Pt bottom electrode and Ti/Al top electrodes, using an imprinting process with molecular monolayers based on bistable rotaxanes do not display characteristic remnant molecular signatures.<sup>[58]</sup> The phenomena observed contrast strikingly with those devices built on a silicon or carbon platform. The voltages required for switching the devices are higher ( $\pm 3.5$  V) and are not stable, displaying a tendency to shift to higher biases as the devices are cycled, generating at each stable ON/OFF state switching amplitudes of anywhere between  $10^3$  and  $10^4$ . The silicon or carbon electrode-based molecular-directed devices, however, switch at the same bias each time, generating more modest switching amplitudes of less than 10. This behaviour is temperature-dependent with none of the switches operating below 200 K, and when they are switched to the ON state they display a volatility associated with relaxation back to the OFF state on the order of 10–60 min. By contrast, for the bimetallic devices, no temperature dependence or volatility is observed. Moreover, these devices display the same behaviour irrespective of the molecule's nature—degenerate catenanes and the dumbbell components of the rotaxanes switch as well as simple amphiphiles. In contrast, for devices made with a silicon or carbon bottom electrode that match closely the position in the periodic table to the molecules, only *bistable* catenanes and rotaxanes display switching. The devices built on Pt display phenomena that can be attributed<sup>[59]</sup> to voltage-driven electromigration of metals piercing through the molecular monolayer, producing an ON state, and retracting back, to produce an OFF state. Such a finding, once again, highlights critically the necessity, when anticipating any new developments in relation to molecule-based nanoelectronics devices, to consider the molecules, the electrodes, and the molecule/electrode interface early on in the design phase of the work.

### Lessons From Molecular Devices

Controllable voltage-driven switching of bistable rotaxanes<sup>[8]</sup> and catenanes<sup>[7,9]</sup> has been demonstrated to occur in a wide range of configurations. Beginning with switching in the solution phase, using either chemical or electrochemical means, these molecular switches were organized next into monolayers at a variety of interfaces. Chemical switching was demonstrated in Langmuir monolayers at the air/water interface and in the LB monolayer counterparts transferred onto silicon substrates. The self-assembled monolayers of rotaxanes on gold, that were electrochemically controlled in a cell resembling a half-device, displayed switching bistability and metastability, the likes of which have only been found so far in silicon- or carbon-based tunnel junction devices. In the

**Table 1. A comparison<sup>A</sup> between devices made with a bottom electrode consisting of silicon and a metallic top electrode**

Ti/Al top electrode poly-Si bottom electrode	Ti/Al top electrode Pt bottom electrode
Switching voltages ( $\pm 2.0$ V) are stable (low bias). (At higher voltages, high bias switching is observed.)	Switching voltages ( $\pm 3.5$ V) are not stable and move to higher values ( $\pm 7$ V) as the devices are cycled (high bias).
Switching amplitudes range between two and ten, depending on the particular bistable molecule and the electrodes.	Switching amplitudes range between $10^3$ and $10^4$ .
Switching behaviour is temperature-dependant and no switch operates below 200 K, indicating that there is an activation barrier.	There is no temperature dependence associated with the switching, indicating that there is no activation barrier.
Switches are volatile, relaxing from the closed to open states in a period of 10–60 min.	Switches are completely non-volatile.
Only bistable catenanes and rotaxanes switch.	All molecules—including degenerate catenanes and dumbbell components of rotaxanes—switch.

<sup>A</sup> The comparison illustrates the importance of considering an electrode–molecule–electrode as a complete and indivisible system.

device arena, molecular electronic devices, based specifically around Si/SiO<sub>2</sub> or CNT bottom electrodes, were fabricated and shown to undergo molecular-based switching of the current between high and low values. Single molecules were transported down to fill a break junction, made from platinum electrodes, to create a device which was found to be dominated by the molecule/metal interfaces and hence revealed the importance of the electrodes' selection. The issue of interfacial transparency was corroborated from devices constructed on a semiconducting carbon nanotube. The last two observations point critically to performing an ensemble assessment of the device's switching and conduction properties, a caveat that was born out in the Pt–molecule–Ti/Al bimetallic devices that display conduction and switching behaviour akin to nanofilamentary growth—and perhaps a viable avenue for molecular electronics to pursue in and of itself.

The growing evidence in favour of nanoelectronics circuitry, with at least some portion deriving its function from molecular elements, provides the impetus to re-evaluate what molecules actually bring to the digital industry and what challenges lie ahead. Moore's Law emerged from the constant theme of technological advancement—enhanced performance at lower cost. It is the drive to this end that provided the motivation to consider molecules as an enabling platform to reach these goals. Molecular size, which ranges from 1 to 100 nm, provides the advantages, which may also be attained one day by nanoscale silicon, of higher density, efficiency, and power dissipation with lower cost. However, molecules display features where there are few parallels in the current semiconductor systems. Molecules can be designed with intermolecular recognition motifs for their self-assembly into nanoscale patterns. Molecules have internal structures, which are coupled to their electronic states, that can be stimulated and thus controlled in a dynamic way for modulation of, in this case, electron transport—that is, function follows structure. Finally, molecules display a synthetic maneuverability that allows them to be custom-built, tuned, and enhanced to fit a variety of boundary conditions and applications. Molecules have the ability to confer unique physical properties, not heretofore seen or as yet anticipated,

in the electronics industry. Nevertheless, the field is very much in its infancy as demonstrated by the variety of phenomena surveyed in this review, even when using the same class of compounds.

The development of molecular electronic devices represents an exemplary part of a holistic approach toward a new paradigm of computers built around molecules, that is, advances in molecular design have been guided by the standards set by the devices and vice versa. Devices were fabricated to accommodate some of the quirks of the molecules. In fact, the recent evolution (Fig. 16) in the structures of interlocked molecules since 1999 is a testament to this interplay. For example, amphiphilicity allowed LB formation for easy monolayer transfer into a device, while electrodes comprised of those elements in the periodic table that are aligned to carbon are much preferred.

An integrated systems-oriented approach permits the various components of molecular electronics—such as design and synthesis of molecular switches, computer architecture development, device design, chemical assembly, and circuit multiplexing<sup>[60]</sup>—to be pursued at one and the same time.

### Future Outlook

Given that the place of molecular switches in memory chips represents a first proof-of-principle demonstration for the applicability for bistable catenanes and rotaxanes in integrated systems, attention can now be turned toward improving their performance. In particular, there are some characteristics of the devices, which, based on the proposed mechanism of switching and conduction, are believed to arise from specific properties of the molecules. (a) ON/OFF current ratios and the absolute current may be increased by using computational models to screen for the effect of exchanging different donor/acceptor components into the switches. (b) The lifetime of the metastable state allows for the memory bits to retain their state with only a single writing voltage, thus minimizing power costs. Consequently, thermodynamic and kinetic parameters associated with the donor/acceptor pairs, as well as the length and nature of the spacer unit separating

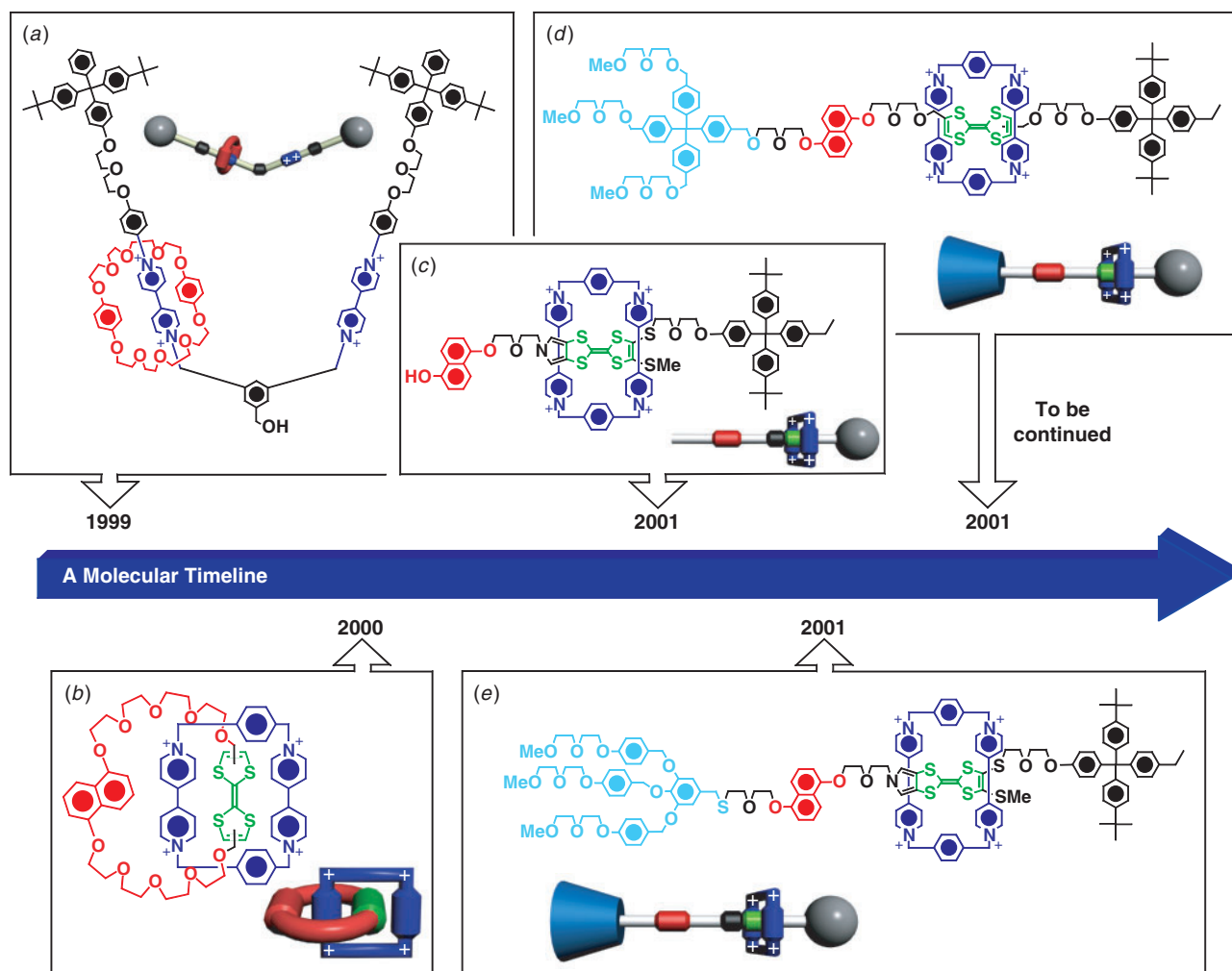


**Fig. 16.** A timeline outlining the evolution of the mechanically interlocked molecules that have been employed so far in electronic devices. The rapid progress in recent years reflects the integrated systems-oriented approach that guided the design of molecular switches and devices alike from the very beginning. (a) The first device was essentially a fuse, but provided the knowledge to construct (b) the first molecular electronic switching device from a bistable [2]catenane. (c) The recognition motifs were modified ever so slightly and the catenane structure was unfurled into a pseudorotaxane-based device and ultimately into bistable [2]rotaxanes, (d) a first-generation one containing a pyrrolo-TTF unit, and (e) a second-generation one incorporating a simple TTF unit.

them can be tuned to optimize the lifetime of the metastable state.

Furthermore, while it is tempting to outline how the systems presented in this review compare with current silicon-based CMOS (complementary metal oxide semiconductor) technology, it is neither so straightforward nor, in our view, a valuable exercise to perform. While initial products bearing molecular technology are likely to lie in niche applications, it is more critical, at least in the research arena, to demonstrate what is possible rather than what is real.

The blueprint for putting some of the world's tiniest machines to work in electronic devices was formed through the close interaction of synthetic chemists with device builders. It is our belief that the same philosophy holds equally well for the emergence of advanced technologies out of fundamental nanoscience. It was this interaction that saw the development of molecular switches take on another dimension and broaden their applicability. The next steps in molecular electronics are likely to be in logic, whereas

the utility of molecular machines is expected to spread to the realm of mechanical manipulation. At present, single-molecule actuators for fundamental studies and palindromically fashioned molecular muscles are being developed and harnessed to perform larger micron- and meso-scale work.

## Conclusions

64-Bit memory chips have been fabricated by integrating molecular switches based on the class of bistable [2]rotaxanes in between crossbars that are defined by Si bottom electrodes and Ti/Al top electrodes. Exploring the opportunities for miniaturization, a binary switching device based on a [2]catenane and a single semiconducting carbon nanotube has been demonstrated. Top-down and bottom-up approaches were hybridized to advance the research program. Molecular switches, based on bistable [2]catenanes and [2]rotaxanes, were first optimized in solution in order to maximize nanometer positional and motion control over the

interlocking molecular components. The catenanes and rotaxanes were customized with amphiphilicity for deposition into full-devices that employ Langmuir–Blodgett methods. Irrespective of the exact nature of the bistable molecular switch that was deposited into the devices based on a silicon or carbon electrode, all of the  $I$ – $V$  measurements were qualitatively identical and repeatable. A self-consistent nanoelectromechanical switching mechanism, based on the solution-phase voltage-gated relative molecular movements, has been proposed and supported by control experiments, half-device models, and computational simulation. Specifically, control studies based on non-switchable compounds do not display binary device behaviour and so underpin the scientific method of investigation into molecular electronics employed in the research programs discussed in this review. Half-devices, based on Langmuir–Blodgett double layers of bistable amphiphilic [2]rotaxanes, show chemically driven redox-activated mechanical switching of the ring's position. Electrode-bound bistable [2]rotaxanes display voltage-gated switching based on the presence of a metastable state of limited lifetime that can be erased using a negative bias in a manner similar to that demonstrated in the full-device. The computational model supports the proposal that the high and low conductance states correspond to the translational isomers where the CBPQT<sup>4+</sup> ring is localized, respectively, on the DNP and TTF recognition sites. Moreover, the shift in the calculated HOMO energy level of the bistable [2]rotaxane is consistent with the experimental behaviour observed from electrochemical measurements in solution and in half-devices. In contrast to these consistencies, measurements on devices, in which both electrodes are metallic, display behaviour that is quite independent of the molecular switches' internal electronic structure, yet may provide an unexpected source of nanoelectronic devices. Therefore, it is important, when employing bistable catenane and rotaxane switches in solid-state devices, for at least one of the electrodes to have a matching work function. Based on the array of studies employed and the approaches used, the development of nanotechnologies may be facilitated within a culture where cross-disciplinary challenges are met head-on by employing an integrated systems-oriented approach.

### Acknowledgements

We would like to acknowledge the involvement of our many collaborators over the past ten years that have contributed greatly to the range of studies and insights gained in the molecular electronics research program presented in this review. The research reported was supported by the Defense Advanced Research Projects Agency (DARPA) and the National Science Foundation (NSF).

### References

- [1] (a) J. F. Stoddart, *Chem. Aust.* **1992**, *59*, 576.  
(b) M. Gómez-López, J. A. Preece, J. F. Stoddart, *Nanotechnology* **1996**, *7*, 183. doi:10.1088/0957-4484/7/3/004  
(c) V. Balzani, M. Gómez-López, J. F. Stoddart, *Acc. Chem. Res.* **1998**, *31*, 405. doi:10.1021/AR970340Y
- (d) V. Balzani, A. Credi, F. M. Raymo, J. F. Stoddart, *Angew. Chem. Int. Ed.* **2000**, *39*, 3348. doi:10.1002/1521-3773(20001002)39:19<3348::AID-ANIE3348>3.0.CO;2-X
- (e) H.-R. Tseng, J. F. Stoddart, in *Modern Arene Chemistry* (Ed. D. Astruc) **2002**, p. 574 (Wiley-VCH: Weinheim).
- [2] (a) A. Harada, *Acc. Chem. Res.* **2001**, *34*, 456. doi:10.1021/AR000174L  
(b) C. A. Schalley, K. Beizai, F. Vögtle, *Acc. Chem. Res.* **2001**, *34*, 465. doi:10.1021/AR000179I  
(c) J.-P. Collin, C. Dietrich-Buchecker, P. Gaviña, M. C. Jimenez-Molero, J.-P. Sauvage, *Acc. Chem. Res.* **2001**, *34*, 477. doi:10.1021/AR0001766  
(d) R. Ballardini, V. Balzani, A. Credi, M. T. Gandolfi, M. Venturi, *Struct. Bonding* **2001**, *99*, 55.  
(e) C. A. Stanier, S. J. Alderman, T. D. W. Claridge, H. L. Anderson, *Angew. Chem. Int. Ed.* **2002**, *41*, 1769. doi:10.1002/1521-3773(20020517)41:10<1769::AID-ANIE1769>3.0.CO;2-N  
(f) V. Balzani, A. Credi, M. Venturi, *Chem. Eur. J.* **2002**, *8*, 5524. doi:10.1002/1521-3765(20021216)8:24<5524::AID-CHEM5524>3.0.CO;2-J  
(g) V. Balzani, A. Credi, M. Venturi, *Molecular Devices and Machines—A Journey into the Nano World* **2003** (Wiley-VCH: Weinheim).
- [3] (a) V. Balzani, A. Credi, F. M. Raymo, J. F. Stoddart, *Angew. Chem. Int. Ed.* **2000**, *39*, 3348. doi:10.1002/1521-3773(20001002)39:19<3348::AID-ANIE3348>3.0.CO;2-X  
(b) B. L. Feringa, *Acc. Chem. Res.* **2001**, *34*, 504. doi:10.1021/AR000172I  
(c) B. L. Feringa, R. A. van Delden, M. K. J. ter Wiel, *Pure Appl. Chem.* **2003**, *75*, 563.
- [4] J. P. Collin, C. Dietrich-Buchecker, P. Gaviña, M. C. Jimenez-Molero, J.-P. Sauvage, *Acc. Chem. Res.* **2001**, *34*, 477. doi:10.1021/AR0001766
- [5] D. A. Leigh, J. K. Y. Wong, F. Dehez, F. Zerbetto, *Nature* **2003**, *424*, 174. doi:10.1038/NATURE01758
- [6] V. Balzani, M. Gómez-López, J. F. Stoddart, *Acc. Chem. Res.* **1998**, *31*, 405. doi:10.1021/AR970340Y
- [7] C. P. Collier, G. Mattersteig, E. W. Wong, Y. Luo, K. Beverly, J. Sampaio, F. M. Raymo, J. F. Stoddart, J. R. Heath, *Science* **2000**, *289*, 1172. doi:10.1126/SCIENCE.289.5482.1172
- [8] (a) E. W. Wong, C. P. Collier, M. Behloradsky, F. M. Raymo, J. F. Stoddart, J. R. Heath, *J. Am. Chem. Soc.* **2000**, *122*, 5831. doi:10.1021/JA993890V  
(b) C. P. Collier, J. O. Jeppesen, Y. Luo, J. Perkins, E. W. Wong, J. R. Heath, J. F. Stoddart, *J. Am. Chem. Soc.* **2001**, *123*, 12632. doi:10.1021/JA0114456  
(c) Y. Luo, C. P. Collier, J. O. Jeppesen, K. A. Nielsen, E. De Ionno, G. Ho, J. Perkins, H.-R. Tseng, et al., *ChemPhysChem* **2002**, *3*, 519. doi:10.1002/1439-7641(20020617)3:6<519::AID-CPHC519>3.0.CO;2-2
- [9] M. R. Diehl, D. W. Steuerman, H.-R. Tseng, S. A. Vignon, A. Star, P. C. Celestre, J. F. Stoddart, J. R. Heath, *ChemPhysChem* **2003**, *4*, 1335. doi:10.1002/CPHC.200300871
- [10] N. A. Melosh, A. Boukai, F. Diana, B. Gerardot, A. Badolato, P. M. Petroff, J. R. Heath, *Science* **2003**, *300*, 112. doi:10.1126/SCIENCE.1081940
- [11] (a) M. A. Reed, C. Zhou, C. J. Muller, T. P. Burgin, J. M. Tour, *Science* **1997**, *278*, 252. doi:10.1126/SCIENCE.278.5336.252  
(b) J. Chen, M. A. Reed, A. M. Rawlett, J. M. Tour, *Science* **1999**, *286*, 1550. doi:10.1126/SCIENCE.286.5444.1550  
(c) C. Li, D. H. Zhang, X. L. Liu, S. Han, T. Tang, C. W. Zhou, W. Fan, J. Koehne, et al., *Appl. Phys. Lett.* **2003**, *82*, 645. doi:10.1063/1.1541943
- [12] (a) D. T. Gryko, C. Clausen, K. M. Roth, N. Dontha, D. F. Bocian, W. G. Kuhr, J. S. Lindsey, *J. Org. Chem.* **2000**, *65*, 7345. doi:10.1021/JO000487U

- (b) D. T. Gryko, F. Zhao, A. A. Yasseri, K. M. Roth, D. F. Bocian, W. G. Kuhr, J. S. Lindsey, *J. Org. Chem.* **2000**, *65*, 7356. doi:10.1021/JO0004862
- (c) C. Clausen, D. T. Gryko, R. B. Dabke, N. Dontha, D. F. Bocian, W. G. Kuhr, J. S. Lindsey, *J. Org. Chem.* **2000**, *65*, 7363. doi:10.1021/JO000488M
- (d) C. Clausen, D. T. Gryko, A. A. Yasseri, J. R. Diers, D. F. Bocian, W. G. Kuhr, J. S. Lindsey, *J. Org. Chem.* **2000**, *65*, 7371. doi:10.1021/JO000489E
- (e) J. Z. Li, D. Gryko, R. B. Dabke, J. R. Diers, D. F. Bocian, W. G. Kuhr, J. S. Lindsey, *J. Org. Chem.* **2000**, *65*, 7379. doi:10.1021/JO000490D
- (f) K. M. Roth, N. Dontha, R. B. Dabke, D. T. Gryko, C. Clausen, J. S. Lindsey, D. F. Bocian, W. G. Kuhr, *J. Vac. Sci. Technol. B* **2000**, *18*, 2359. doi:10.1116/1.1310657
- (g) K. M. Roth, D. T. Gryko, C. Clausen, J. Z. Li, J. S. Lindsey, W. G. Kuhr, D. F. Bocian, *J. Phys. Chem. B* **2002**, *106*, 8639. doi:10.1021/JP025850A
- (h) Q. L. Li, G. Mathur, M. Homsy, S. Surthi, V. Misra, V. Malinovskii, K. H. Schweikart, L. H. Yu, et al., *Appl. Phys. Lett.* **2002**, *81*, 1494. doi:10.1063/1.1500781
- (i) K. M. Roth, J. S. Lindsey, D. F. Bocian, W. G. Kuhr, *Langmuir* **2002**, *18*, 4030. doi:10.1021/LA025525E
- (j) K. H. Schweikart, V. L. Malinovskii, J. R. Diers, A. A. Yasseri, D. F. Bocian, W. G. Kuhr, J. S. Lindsey, *J. Mater. Chem.* **2002**, *12*, 808. doi:10.1039/B108520D
- (k) Q. L. Li, S. Surthi, G. Mathur, S. Gowda, V. Misra, T. A. Sorenson, R. C. Tenent, W. G. Kuhr, et al., *Appl. Phys. Lett.* **2003**, *83*, 198. doi:10.1063/1.1584088
- [13] K. M. Roth, A. A. Yasseri, Z. M. Liu, R. B. Dabke, V. Malinovskii, K. H. Schweikart, L. H. Yu, H. Tiznado, et al., *J. Am. Chem. Soc.* **2003**, *125*, 505. doi:10.1021/JA021169A
- [14] (a) C. R. Kagan, D. B. Mitzi, C. D. Dimitrakopoulos, *Science* **1999**, *286*, 945. doi:10.1126/SCIENCE.286.5441.945
- (b) D. B. Mitzi, K. Chondroudis, C. R. Kagan, *IBM J. Res. Dev.* **2001**, *45*, 29.
- (c) C. R. Kagan, A. Afzali, R. Martel, L. M. Gignac, P. M. Solomon, A. G. Schrott, B. Ek, *Nano Lett.* **2003**, *3*, 119. doi:10.1021/NL0259075
- [15] (a) S. H. Chanteau, J. M. Tour, *Tetrahedron Lett.* **2001**, *42*, 3057. doi:10.1016/S0040-4039(01)00394-X
- (b) S. M. Dirk, D. W. Price, S. Chanteau, D. V. Kosynkin, J. M. Tour, *Tetrahedron* **2001**, *57*, 5109. doi:10.1016/S0040-4020(01)00361-1
- (c) Z. J. Donhauser, B. A. Mantooh, K. F. Kelly, L. A. Bumm, J. D. Monnell, J. J. Stapleton, D. W. Price, A. M. Rawlett, et al., *Science* **2001**, *292*, 2303. doi:10.1126/SCIENCE.1060294
- (d) A. Reed, J. Chen, A. M. Rawlett, D. W. Price, J. M. Tour, *Appl. Phys. Lett.* **2001**, *78*, 3735. doi:10.1063/1.1377042
- (e) F. R. F. Fan, J. P. Yang, L. T. Cai, D. W. Price, S. M. Dirk, D. V. Kosynkin, Y. X. Yao, A. M. Rawlett, et al., *J. Am. Chem. Soc.* **2002**, *124*, 5550. doi:10.1021/JA017706T
- (f) J. M. Tour, W. L. Van Zandt, C. P. Husband, S. M. Husband, L. S. Wilson, P. D. Franzon, D. P. Nackashi, *IEEE Trans. Nanotechnol.* **2002**, *1*, 100. doi:10.1109/TNANO.2002.804744
- (g) C. P. Husband, S. M. Husband, J. S. Daniels, J. M. Tour, *IEEE Trans. Nanotechnol.* **2003**, *50*, 1865. doi:10.1109/TED.2003.815860
- [16] (a) J. G. Kushmerick, D. B. Holt, J. C. Yang, J. Naciri, M. H. Moore, R. Shashidhar, *Phys. Rev. Lett.* **2002**, *89*.
- (b) J. G. Kushmerick, J. Naciri, J. C. Yang, R. Shashidhar, *Nano Lett.* **2003**, *3*, 897. doi:10.1021/NL034201N
- [17] (a) J. K. N. Mbindyo, N. I. Kovtyukhova, B. Razavi, I. Kratochvilova, S. K. S. Angelo, T. S. Mayer, T. N. Jackson, T. E. Mallouk, *Abstr. Pap. Am. Chem. Soc.* **2002**, *223*, C42.
- (b) J. K. N. Mbindyo, T. E. Mallouk, J. B. Mattzela, I. Kratochvilova, B. Razavi, T. N. Jackson, T. S. Mayer, *J. Am. Chem. Soc.* **2002**, *124*, 4020. doi:10.1021/JA016696T
- [18] (a) T. Rueckes, K. Kim, E. Joselevich, G. Y. Tseng, C. L. Cheung, C. M. Lieber, *Science* **2000**, *289*, 94. doi:10.1126/SCIENCE.289.5476.94
- (b) Y. Cui, Q. Q. Wei, H. K. Park, C. M. Lieber, *Science* **2001**, *293*, 1289. doi:10.1126/SCIENCE.1062711
- (c) C. M. Lieber, *Sci. Am.* **2001**, *285*, 58.
- (d) Y. Cui, C. M. Lieber, *Science* **2001**, *291*, 851. doi:10.1126/SCIENCE.291.5505.851
- (e) Y. Huang, X. F. Duan, Q. Q. Wei, C. M. Lieber, *Science* **2001**, *291*, 630. doi:10.1126/SCIENCE.291.5504.630
- (f) Y. Huang, X. F. Duan, Y. Cui, L. J. Lauhon, K. H. Kim, C. M. Lieber, *Science* **2001**, *294*, 1313. doi:10.1126/SCIENCE.1066192
- (g) Y. Huang, X. F. Duan, Y. Cui, C. M. Lieber, *Nano Lett.* **2002**, *2*, 101. doi:10.1021/NL015667D
- (h) C. M. Lieber, *Nano Lett.* **2002**, *2*, 81. doi:10.1021/NL020289D
- (i) X. F. Duan, Y. Huang, C. M. Lieber, *Nano Lett.* **2002**, *2*, 487. doi:10.1021/NL025532N
- [19] (a) A. Javey, H. Kim, M. Brink, Q. Wang, A. Ural, J. Guo, P. McIntyre, P. McEuen, et al., *Nat. Mater.* **2002**, *1*, 241. doi:10.1038/NMAT769
- (b) A. Javey, Q. Wang, A. Ural, Y. M. Li, H. J. Dai, *Nano Lett.* **2002**, *2*, 929. doi:10.1021/NL025647R
- (c) N. R. Franklin, Q. Wang, T. W. Tomblor, A. Javey, M. Shim, H. J. Dai, *Appl. Phys. Lett.* **2002**, *81*, 913. doi:10.1063/1.1497710
- (d) Y. Kim, A. Javey, O. Vermesh, O. Wang, Y. M. Li, H. J. Dai, *Nano Lett.* **2003**, *3*, 193. doi:10.1021/NL0259232
- (e) A. Javey, J. Guo, Q. Wang, M. Lundstrom, H. J. Dai, *Nature* **2003**, *424*, 654. doi:10.1038/NATURE01797
- [20] C. P. Collier, E. W. Wong, M. Belohradsky, F. M. Raymo, J. F. Stoddart, P. J. Kuekes, R. S. Williams, J. R. Heath, *Science* **1999**, *285*, 391. doi:10.1126/SCIENCE.285.5426.391
- [21] T. L. J. Chen, J. Su, W. Wang, M. A. Reed, A. M. Rawlett, M. Kozaki, Y. Yao, R. C. Jagessar, et al., *Molecular Nanoelectronics* (Eds M. A. Reed, T. Lee) **2003** (American Scientific Publishers: Stevenson Ranch, CA).
- [22] R. M. Metzger, *Chem. Rev.* **2003**, *103*, 3803. doi:10.1021/CR020413D
- [23] B. Odell, M. V. Reddington, A. M. Z. Slawin, N. Spencer, J. F. Stoddart, D. J. Williams, *Angew. Chem. Int. Ed. Engl.* **1988**, *27*, 1547. doi:10.1002/ANIE.198815471
- [24] (a) J. M. Lehn, *Angew. Chem. Int. Ed. Engl.* **1988**, *27*, 89. doi:10.1002/ANIE.198800891
- (b) C. J. Pedersen, *Angew. Chem. Int. Ed. Engl.* **1988**, *27*, 1021. doi:10.1002/ANIE.198810211
- [25] D. J. Cram, *Angew. Chem. Int. Ed. Engl.* **1988**, *27*, 1009. doi:10.1002/ANIE.198810093
- [26] (a) M. C. T. Fyfe, J. F. Stoddart, *Acc. Chem. Res.* **1997**, *30*, 393. doi:10.1021/AR950199Y
- (b) H.-J. Schneider, A. Yatsimisky, *Principles and Methods in Supramolecular Chemistry 2000* (Wiley-VCH: Weinheim).
- (c) J. W. Steed, J. L. Atwood, *Supramolecular Chemistry 2000* (Wiley-VCH: Weinheim).
- (d) D. N. Reinhoudt, M. Crego-Calama, *Science* **2002**, *295*, 2403. doi:10.1126/SCIENCE.1069197
- (e) G. M. Whitesides, B. Grzybowski, *Science* **2002**, *295*, 2418. doi:10.1126/SCIENCE.1070821
- [27] P. R. Ashton, B. Odell, M. V. Reddington, A. M. Z. Slawin, J. F. Stoddart, D. J. Williams, *Angew. Chem. Int. Ed. Engl.* **1988**, *27*, 1550. doi:10.1002/ANIE.198815501
- [28] P. R. Ashton, T. T. Goodnow, A. E. Kaifer, M. V. Reddington, A. M. Z. Slawin, N. Spencer, J. F. Stoddart, C. Vicent, D. J. Williams, *Angew. Chem. Int. Ed. Engl.* **1989**, *28*, 1396. doi:10.1002/ANIE.198913961
- [29] D. B. Amabilino, P. R. Ashton, A. S. Reder, N. Spencer, J. F. Stoddart, *Angew. Chem. Int. Ed. Engl.* **1994**, *33*, 1286. doi:10.1002/ANIE.199412861

- [30] (a) *Molecular Catenanes, Rotaxanes and Knots* (Eds J.-P. Sauvage, C. O. Dietrich-Buchecker) **1999** (Wiley-VCH: Weinheim).  
(b) G. Schill, *Catenanes, Rotaxanes, and Knots* **1971** (Academic Press: New York, NY).
- [31] P.-L. Anelli, N. Spencer, J. F. Stoddart, *J. Am. Chem. Soc.* **1991**, *113*, 5131.
- [32] R. A. Bissell, E. Córdova, A. E. Kaifer, J. F. Stoddart, *Nature* **1994**, *369*, 133. doi:10.1038/369133A0
- [33] R. Ballardini, V. Balzani, J. Becher, A. Di Fabio, M. T. Gandolfi, G. Matternsteig, M. B. Nielsen, F. M. Raymo, et al., *J. Org. Chem.* **2000**, *65*, 4120. doi:10.1021/JO000194I
- [34] J.-P. Collin, P. Gavina, J.-P. Sauvage, *New J. Chem.* **1997**, *21*, 525.
- [35] A. Livoreil, C. O. Dietrich-Buchecker, J.-P. Sauvage, *J. Am. Chem. Soc.* **1994**, *116*, 9399.
- [36] (a) L. Raehm, J.-M. Kern, J.-P. Sauvage, *Chem. Eur. J.* **1999**, *5*, 3310. doi:10.1002/(SICI)1521-3765(19991105)5:11<3310::AID-CHEM3310>3.0.CO;2-R  
(b) L. Raehm, J.-M. Kern, J.-P. Sauvage, C. Hamann, S. Palacin, J.-P. Bourgoin, *Chem. Eur. J.* **2002**, *8*, 2153. doi:10.1002/1521-3765(20020503)8:9<2153::AID-CHEM2153>3.0.CO;2-E
- [37] M. D. Asakawa, W. Dehaem, G. L'abbé, S. Menzer, J. Nouwen, F. M. Raymo, J. F. Stoddart, D. J. Williams, *J. Org. Chem.* **1996**, *61*, 9591. doi:10.1021/JO961488I
- [38] (a) M. Asakawa, P. R. Ashton, V. Balzani, A. Credi, G. Matternsteig, O. A. Matthews, M. Montalti, N. Spencer, et al., *Chem. Eur. J.* **1997**, *3*, 1992.  
(b) A. Credi, M. Montalti, V. Balzani, S. J. Langford, F. M. Raymo, J. F. Stoddart, *New J. Chem.* **1998**, *22*, 1061. doi:10.1039/A804787A  
(c) M. Asakawa, P. R. Ashton, V. Balzani, S. E. Boyd, A. Credi, G. Matternsteig, S. Menzer, M. Montalti, et al., *Eur. J. Org. Chem.* **1999**, 985. doi:10.1002/(SICI)1099-0690(199905)1999:5<985::AID-EJOC985>3.0.CO;2-O  
(d) P. R. Ashton, V. Balzani, J. Becher, A. Credi, M. C. T. Fyfe, G. Matternsteig, S. Menzer, M. B. Nielsen, et al., *J. Am. Chem. Soc.* **1999**, *121*, 3951. doi:10.1021/JA984341C  
(e) V. Balzani, A. Credi, G. Matternsteig, O. A. Matthews, F. M. Raymo, J. F. Stoddart, M. Venturi, A. J. P. White, et al., *J. Org. Chem.* **2000**, *65*, 1924. doi:10.1021/JO991781T  
(f) P. R. Ashton, V. Balzani, V. Balzani, A. Credi, H. D. A. Hoffmann, M. V. Martín-Díaz, F. M. Raymo, J. F. Stoddart, et al., *Chem. Eur. J.* **2001**, *7*, 3482. doi:10.1002/1521-3765(20010817)7:16<3482::AID-CHEM3482>3.0.CO;2-G  
(g) R. Ballardini, V. Balzani, A. Di Fabio, M. T. Gandolfi, J. Becher, J. Lau, M. B. Nielsen, J. F. Stoddart, *New J. Chem.* **2001**, *25*, 293. doi:10.1039/B007836K  
(h) T. Yamamoto, H.-R. Tseng, J. F. Stoddart, V. Balzani, A. Credi, F. Marchioni, M. Venturi, *Collect. Czech. Chem. Commun.* **2003**, *68*, 1488. doi:10.1135/CCCC20031488
- [39] A. Ulman, *An Introduction to Ultrathin Organic Films from Langmuir-Blodgett to Self-Assembly* **1991** (Academic Press: San Diego, CA).
- [40] J. O. Jeppesen, J. Perkins, J. Becher, J. F. Stoddart, *Angew. Chem. Int. Ed.* **2001**, *40*, 1216. doi:10.1002/1521-3773(20010401)40:7<1216::AID-ANIE1216>3.3.CO;2-N
- [41] I. C. Lee, C. W. Frank, T. Yamamoto, H.-R. Tseng, A. H. Flood, J. F. Stoddart, J. O. Jeppesen, *Langmuir*, in press.
- [42] M. Asakawa, P. R. Ashton, V. Balzani, A. Credi, C. Hamers, G. Matternsteig, M. Montalti, A. N. Shipway, et al., *Angew. Chem. Int. Ed.* **1998**, *37*, 333. doi:10.1002/(SICI)1521-3773(19980216)37:3<333::AID-ANIE333>3.0.CO;2-P
- [43] H.-R. Tseng, S. A. Vignon, J. F. Stoddart, *Angew. Chem. Int. Ed.* **2003**, *42*, 1491. doi:10.1002/ANIE.200250453
- [44] M. Asakawa, M. Higuchi, G. Matternsteig, T. Nakamura, A. R. Pease, F. M. Raymo, T. Shimizu, J. F. Stoddart, *Adv. Mater.* **2000**, *12*, 1099. doi:10.1002/1521-4095(200008)12:15<1099::AID-ADMA1099>3.0.CO;2-2
- [45] H.-R. Tseng, D. Wu, N. X. Fang, X. Zhang, J. F. Stoddart, *ChemPhysChem* **2004**, *5*, 111. doi:10.1002/CPHC.200300992
- [46] H.-R. Tseng, S. A. Vignon, P. C. Celestre, J. Perkins, A. Di Fabio, R. Ballardini, M. T. Gandolfi, M. Venturi, et al., *Chem. Eur. J.* **2004**, *10*, 155. doi:10.1002/CHEM.200305204
- [47] S. Kang, S. A. Vignon, H.-R. Tseng, J. F. Stoddart, *Chem. Eur. J.* **2004**, in press.
- [48] M. E. Lines, A. M. Glass, *Properties and Applications of Ferroelectrics and Related Materials* **1977** (Clarendon: Oxford).
- [49] W. Deng, R. P. Muller, W. A. Goddard, unpublished results. See also a report on 'Computational Nanotechnology' by E. K. Wilson, *Chem. Eng. News* **2003**, April 28, 27–29.
- [50] J. R. Heath, M. A. Ratner, *Phys. Today* **2003**, *56*, 43.
- [51] A. C. Benniston, A. Harriman, D. Philp, J. F. Stoddart, *J. Am. Chem. Soc.* **1993**, *115*, 5298.
- [52] H. Yu, Y. Luo, K. Beverly, H.-R. Tseng, J. F. Stoddart, J. R. Heath, *Angew. Chem. Int. Ed.* **2003**, *42*, 5706. doi:10.1002/ANIE.200352352
- [53] (a) H. Park, J. Park, A. K. L. Lim, E. H. Anderson, A. P. Alivisatos, P. L. McEuen, *Nature* **2000**, *407*, 57. doi:10.1038/35024031  
(b) J. W. Park, A. N. Pasupathy, J. I. Goldsmith, A. V. Soldatov, C. Chang, Y. Yaish, J. P. Sethna, H. D. Abruña, et al., *Thin Solid Films* **2003**, *438–439*, 457. doi:10.1016/S0040-6090(03)00805-8
- [54] At 4 K, any movements of the CBPQT<sup>4+</sup> ring are expected to be frozen out. Given the dominance of the surface states due to the molecule's attachment, further studies with control compounds that mimic the ON state were not investigated.
- [55] (a) R. C. Ahuja, P. L. Caruso, D. Mobius, G. Wildburg, H. Ringsdorf, D. Philp, J. A. Preece, J. F. Stoddart, *Langmuir* **1993**, *9*, 1534.  
(b) R. C. Ahuja, P. L. Caruso, D. Mobius, D. Philp, J. A. Preece, H. Ringsdorf, J. F. Stoddart, G. Wildburg, *Thin Solid Films* **1996**, *284–285*, 671. doi:10.1016/S0040-6090(95)08418-5  
(c) C. L. Brown, U. Jonas, J. A. Preece, H. Ringsdorf, M. Seitz, J. F. Stoddart, *Langmuir* **2000**, *16*, 1924. doi:10.1021/LA990791M
- [56] J. Kong, N. R. Franklin, C. W. Zhou, M. G. Chapline, S. Peng, K. J. Cho, H. J. Dai, *Science* **2000**, *287*, 622. doi:10.1126/SCIENCE.287.5453.622
- [57] (a) P. R. Ashton, S. E. Boyd, A. Brindle, S. J. Langford, S. Menzer, L. Pérez-García, J. A. Preece, F. M. Raymo, et al., *New J. Chem.* **1999**, *23*, 587. doi:10.1039/A809433K  
(b) V. Balzani, A. Credi, S. J. Langford, F. M. Raymo, J. F. Stoddart, M. Venturi, *J. Am. Chem. Soc.* **2000**, *122*, 3542. doi:10.1021/JA994454B
- [58] Y. Chen, D. A. A. Ohlberg, X. M. Li, D. R. Stewart, R. S. Williams, J. O. Jeppesen, K. A. Nielsen, J. F. Stoddart, et al., *Appl. Phys. Lett.* **2003**, *82*, 1610. doi:10.1063/1.1559439
- [59] D. R. Stewart, D. A. A. Ohlberg, P. A. Beck, Y. Chen, R. S. Williams, J. O. Jeppesen, K. A. Nielsen, J. F. Stoddart, *Nano Lett.* **2004**, *4*, 133. doi:10.1021/NL034795U
- [60] Y. Chen, G. Y. Jung, D. A. A. Ohlberg, X. M. Li, D. R. Stewart, J. O. Jeppesen, K. A. Nielsen, J. F. Stoddart, R. S. Williams, *Nanotechnology* **2003**, *14*, 462. doi:10.1088/0957-4484/14/4/311